



저작자표시-비영리-변경금지 2.0 대한민국

이용자는 아래의 조건을 따르는 경우에 한하여 자유롭게

- 이 저작물을 복제, 배포, 전송, 전시, 공연 및 방송할 수 있습니다.

다음과 같은 조건을 따라야 합니다:



저작자표시. 귀하는 원저작자를 표시하여야 합니다.



비영리. 귀하는 이 저작물을 영리 목적으로 이용할 수 없습니다.



변경금지. 귀하는 이 저작물을 개작, 변형 또는 가공할 수 없습니다.

- 귀하는, 이 저작물의 재이용이나 배포의 경우, 이 저작물에 적용된 이용허락조건을 명확하게 나타내어야 합니다.
- 저작권자로부터 별도의 허가를 받으면 이러한 조건들은 적용되지 않습니다.

저작권법에 따른 이용자의 권리는 위의 내용에 의하여 영향을 받지 않습니다.

이것은 [이용허락규약\(Legal Code\)](#)을 이해하기 쉽게 요약한 것입니다.

[Disclaimer](#)

Doctor of Philosophy

Hepatic differentiation and regeneration potential of  
mesenchymal stem cells in xeno-free conditions

중간엽 줄기세포를 이용한  
간세포 분화와 치료기전 연구

The Graduate School  
of the University of Ulsan

Department of Medical science

Jiwan Choi

Hepatic differentiation and regeneration potential of  
mesenchymal stem cells in xeno-free conditions

Supervisor Sang-Eun Lee

A Dissertation

Submitted to  
the Graduate School of the University of Ulsan  
In partial Fulfilment of the Requirements  
for the Degree of

Doctor of Philosophy

By

Ji-wan Choi

Department of Medical science  
University of Ulsan, Korea  
February 2022

This certifies that the dissertation  
of Jiwan Choi is approved.



---

Committee Chair Dr. Soo Jin Oh



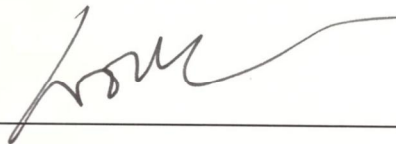
---

Committee Member Dr. Sang-Eun Lee



---

Committee Member Dr. Eunju Kang



---

Committee Member Dr. Young Hoon Sung



---

Committee Member Dr. Chang Mo Hwang

Department of Medical science  
University of Ulsan, Korea

February 2022

## 국문 요약

간은 사람 신체 내에서 중심에 자리 잡고 있으며, 약물, 화학물의 분해와 외부에서 들어오는 독성을 해독하며, 몸에 필요한 다양한 물질을 합성하는 중요한 장기이다. 오늘 날, 미국에서만 10 만명 이상의 간질환 환자가 발생하고 있으며, 그 중 12,000 명이 매년 간질환으로 인해 사망한다고 하며, 한국에서도 2018 년도 통계에 따르면 간질환으로 사망한 사람의 수가 전체 사망자 수의 7 위에 해당한다고 한다. 이렇게 간질환으로 인해 사망하는 사람의 수가 많은 이유는 심각한 간 질환을 가진 환자들의 대부분의 치료법으로 간 이식을 통해서만 병을 치료할 수 있기 때문이다. 하지만 이식할 수 있는 간 조직의 공급은 수요에 비해 부족하며, 장기 이식 후 나타나는 다양한 거부 반응, 이식 후 면역억제제 복용에 따른 부작용 등으로 인해 이식 수술을 대체할 재생 치료제의 개발 필요성이 대두되고 있다.

최근 줄기세포를 이용한 치료 기술의 발전으로 인해 줄기세포를 이용한 치료법 개발이 활발히 일어나고 있으며, 다양한 조직에서 유래한 줄기세포를 원하는 조직 세포 (피부, 연골, 심장세포 등)로 분화하여 이를 치료제로 사용하려는 세포 치료제 연구가 진행되고 있다. 특히, 만능줄기세포 (human induced pluripotent stem cells, hiPSC)와 배아 줄기세포 (human embryonic stem cells, hESC) 등을 이용하여 연구가 진행 중이지만, 이는 체내로 들어갔을 때, 암화가 진행 될 수 있으며, 이를 조절할 수 없기에 안정성이 떨어진다는 연구결과가 나오고 있다. 따라서 현재 안정성이 검증된 태아 혹은 성체 조직에서 유래한 중간엽 줄기세포 (mesenchymal stem cells, MSC)을 추출하여 필요한 조직으로 유도하고 이식하는 연구가 활발히 진행되고 있다.

본 연구에선 태아에서 얻을 수 있는 제대혈과 양막 유래 줄기세포와 성체에서

연을 수 있는 골수와 간조직 유래 줄기세포를 추출하여 세포의 크기, 분화능력, 면역조절 작용, 미토콘드리아 기능 검사 등을 진행하여 각 유래 별 줄기세포의 특징을 연구하였다. 또한 세포 치료를 위해선 다량의 세포를 확보 하는게 중요한데, 양막 유래 줄기세포는 다량으로 배양할 수 있는 특징을 가지고 있으므로 여기에 잘 들어 맞는 세포임을 밝혔다. 다음으로 이러한 특징들을 종합하여 세포 치료에 가장 유능할 것이라고 생각되어지는 양막 유래 줄기세포를 선택하여 간세포로의 분화를 진행하였다. 특히 본 연구에선 transcriptome 분석을 통해 양막 유래 줄기세포의 유전체 발현 정도를 분석하였다. 양막 유래 줄기세포엔 GATA6의 발현이 낮으며, GSK3의 발현이 높아 간세포로 분화가 어려워, CHIR99021이라는 화학물질을 첨가하여 간세포로의 분화 효율을 올렸다. 특히, 폴리 비닐 알코올 (PVA)라는 이용, 그동안 많은 간 분화를 위해 사용했던 FBS를 대신하여 PVA를 분화에 사용함으로써, 외부 물질이 오염되지 않고 효율적으로 양막 줄기세포를 간세포로 분화할 수 있는 간 분화 프로토콜을 적립하였다. 또한 이 간세포가 알부민을 합성하여 외부로 분비하며, 몸에서 중요한 간 특이 효소로 외부 항원을 분해 한다고 알려진 CYP3A4가 발현하고 활성이 된다는 것도 실험을 통하여 밝혔다. 마지막으로 본 연구에선 안정적인 간질환 마우스 모델을 확립하여 양막 줄기세포에서 분화된 간세포를 이식하고, 치료 효과와 이식 효율 등을 실험하여 성공적으로 양막 줄기세포 유래 간세포가 간질환 마우스 모델에 이식되는 것을 확인하였다.

본 연구는 세포 치료에 유망할 것이라고 생각되어지는 양막 유래 중간엽 줄기세포를 사용하여 간 분화를 진행하였다. 또한 줄기세포의 유전체 분석을 통해 같은 장기의 줄기세포 유래임에도 조금씩 다른 세포 내 기전이 있다는 것을 밝혔다. 또한 유전체 분석을 통해 새롭게 적립한 효율적이고 외부 항원 감염이 없는 간세포 분화 방법을 적립하여 기능이 존재하는 간세포를 줄기세포로부터 분화하였다. 마지막으로 간세포가 임상학

적으로 사용될 수 있는 가능성을 간 질환 동물 모델을 통해 전임상학적으로 제시하였다. 따라서 기능이 있고 이식이 가능한 줄기세포 유래 간 세포 분화 방법을 연구함으로써 앞으로의 간질환 환자의 세포 치료에 일조하고자 하였다.

## Abstract

The liver plays a critical role in the human body, such as detoxification, synthesis, and metabolism. Unfortunately, many people suffer from liver diseases, and the number was increased every year. Recently, stem cell technologies were advanced, and stem cells are expected to replace liver transplantation in the future. Particularly, Mesenchymal stem cells (MSCs) are in the spotlight for cell therapy.

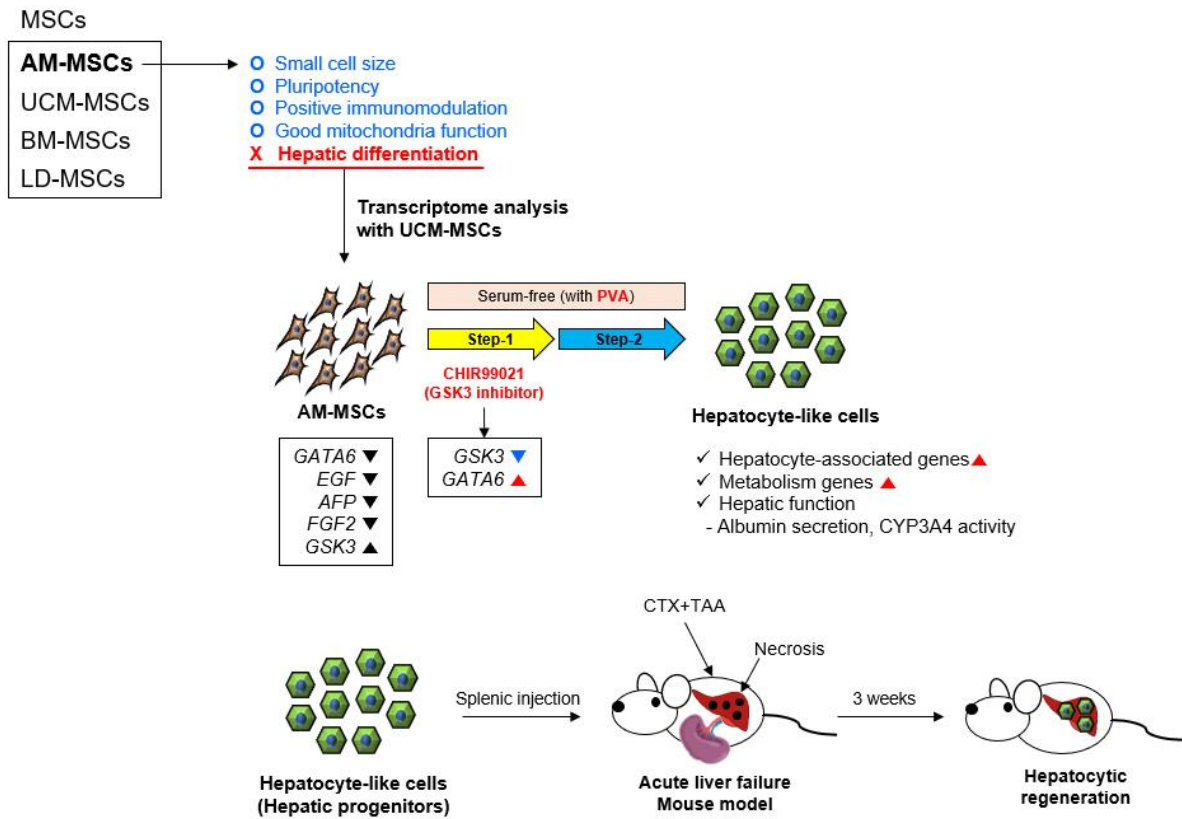
At the beginning of this study, we determined one MSC line that was appropriated for cell therapy and hepatic differentiation through several experiments, such as a measurement of cell size, pluripotency, immunomodulation, and mitochondrial function. As a result, amnion-derived mesenchymal stem cells (AM-MSCs) are a great source of stem cell therapy for patients with liver diseases. However, there are obstacles to their use due to low efficiency and xeno-contamination for hepatic differentiation. Thus, we established an efficient protocol for differentiating AM-MSCs into hepatocyte-like cells (HLCs) by analyzing transcriptome-sequencing data. In AM-MSCs, hepatic development-associated genes, including *GATA6*, *EGF*, *AFP*, and *FGF2* were downregulated, and *GSK3* was upregulated. The high levels of *GSK3* could repress the induction of hepatocytes. Based on this result, we established an efficient hepatic differentiation protocol using the *GSK3* inhibitor, CHIR99021, with various supplements. Moreover, to generate the xeno-free conditioned differentiation protocol, we replaced fetal bovine serum (FBS) with polyvinyl alcohol (PVA). As a result, PVA was improved differentiation ability, such as upregulation of hepatic progenitor, hepatocyte-related, and metabolism markers. Finally, we measured the hepatocyte functions with the expression of gene levels and protein, secretion of albumin, and activity of CYP3A4. The differentiated HLCs not only synthesized and secreted albumin but also metabolized drugs by the CYP3A4 enzyme.

Further, to test the transplantable potential of AM-HLCs, we optimized a transplantation date, 12 days after initiation of differentiation, based on the expression of hepatic progenitor gene and mitochondrial function. Finally, we established a mouse model of acute liver failure using a thioacetamide (TAA) and cyclophosphamide monohydrate (CTX) and transplanted AM-hepatic progenitors (HPCs) in the mouse model through splenic injection. When the AM-HPCs were transplanted into the liver failure mouse model, they settled in the damaged livers and differentiated into hepatocytes. This study offers an efficient and xeno-free conditioned hepatic differentiation protocol and shows that AM-HPCs could be used as transplantable therapeutic materials. Thus, we suggest that AM-MSC-derived HPCs are promising cells for treating liver disease.

**Key words:** Liver, Mesenchymal stem cells, Amniotic membrane, Liver failure, Transplantation



## Graphical summary of the study



# Contents

국문요약.....	1
Abstract.....	4
Contents.....	6
List of Figures.....	9
List of Tables.....	10
List of Abbreviations.....	11

## Chapter I. General Introduction

I-1. Abstract.....	14
<b>I-2. Research Background and Introduction</b>	
I-2-1. The liver.....	15
I-2-2. Liver disease.....	15
I-2-3. Stem cells.....	16
I-2-4. Mesenchymal stem cells.....	17
<b>I-3. Materials and Methods</b>	
I-3-1. Cell isolation.....	19
I-3-2. Cell culture.....	19
I-3-3. Cell surface proteins analysis.....	19
I-3-4. Quantitative RT-qPCR.....	20
I-3-5. Mixed Lymphocyte Reaction assay.....	20
I-3-6. Seahorse assay.....	21
I-3-7. Osteogenesis and adipogenesis of AM-MSCs.....	21
I-3-8. Measuring the cell growth rate.....	21
I-3-9. Production of B2M-KO-AM-MSCs.....	22
I-3-10. Statistical analysis.....	22
<b>I-4. Results</b>	
I-4-1. Phenotypical comparison of human mesenchymal stem cells from the umbilical cord, bone marrow, liver, and amniotic membrane.....	23
I-4-2. Cellular characteristics as human mesenchymal stem cells.....	23

I-4-3. The mass-production potential of AM-MSCs.....	25
I-4-4. Generation of universal cells from AM-MSCs.....	30

**Chapter II. The study of *in vitro* hepatic differentiation**

<b>II-1. Abstract</b> .....	34
<b>II-2. Introduction</b> .....	35
<b>II-3. Materials and Methods</b>	
II-3-1. Quantitative RT-qPCR.....	37
II-3-2. Seahorse assay.....	37
II-3-3. Immunocytochemical staining.....	38
II-3-4. Transcriptome analysis.....	38
II-3-5. <i>In vitro</i> hepatic differentiation.....	38
II-3-6. Culture for primary human hepatocytes.....	39
II-3-7. Detection of secreted human albumin.....	39
II-3-8. Measurement of CYP3A4 activity in vitro using LC-ESI/MS/MS system.....	39
II-3-9. Measurement of CYP3A4 activity in vitro using luminescence system.....	40
II-3-10. Statistical analysis.....	40
<b>II-4. Results</b>	
II-4-1. <i>In vitro</i> hepatic differentiation of four different types of MSC lines.....	41
II-4-2. Transcriptome analysis of AM-MSCs and UCM-MSCs.....	41
II-4-3. Analysis for the efficient hepatic differentiation.....	44
II-4-4. Efficient <i>in vitro</i> hepatic differentiation protocol.....	44
II-4-5. The use of PVA for xeno-free hepatic differentiation.....	47
II-4-6. The hepatic functions of AM-HLCs.....	47
II-4-7. Summary of <i>in vitro</i> hepatic differentiation.....	52

**Chapter III. The study of *in vivo* hepatic transplantation and regeneration**

<b>III-1. Abstract</b> .....	55
<b>III-2. Introduction</b> .....	56
<b>III-3. Materials and Methods</b>	
III-3-1. Transplantation experiments.....	57
III-3-2. Blood analysis.....	57

III-3-3. Histological staining and analysis.....	57
III-3-4. <i>In vitro</i> differentiation of hepatic differentiation.....	57
III-3-5. Immunofluorescence staining.....	58
III-3-6. Human mitochondrial DNA detection.....	58
III-3-7. Evaluation of transplant efficiency.....	58
III-3-8. Statistical analysis.....	59
<b>III-4. Results</b>	
III-4-1. Acute hepatic failure mouse model.....	60
III-4-2. Optimization of transplantation date.....	60
III-4-3. Engraftability of AM-HPCs.....	64
III-4-4. The therapeutic capacity of AM-HPCs.....	64
III-4-5. Summary of <i>in vivo</i> studies.....	64
<b>Discussions</b> .....	69
<b>References</b> .....	73

## List of Figures

Graphical summary.....	5
Figure 1. The phenotype of human mesenchymal stem cells from various organs.....	24
Figure 2. Cellular characteristics of human mesenchymal stem cells.....	26
Figure 3. Mass production of AM-MSCs.....	28
Figure 4. Estimation of total cell numbers during the passage.....	29
Figure 5. Generation of hypo-immune potential universal cells from AM-MSCs.....	31
Figure 6. Phenotypes of hypo-immune potential universal cells from AM-MSCs.....	32
Figure 7. Hepatic generation of human mesenchymal stem cells using the conventional method.....	42
Figure 8. Transcriptome analysis in UCM-MSCs and AM-MSCs.....	43
Figure 9. Enhancing the endoderm differentiation potent based on the transcriptome analysis.....	45
Figure 10. Advanced protocol for enhancing the hepatic differentiation of AM-MSCs.....	46
Figure 11. Serum-free hepatic differentiation using PVA.....	49
Figure 12. The effect of advanced protocol on UCM-MSCs.....	50
Figure 13. The hepatic function of AM-derived hepatocyte-like cells induced by PVA-used protocol.....	51
Figure 14. Schematic summary of in vitro study.....	53
Figure 15. Modification of acute liver failure mouse model.....	62
Figure 16. Optimizing the differentiation date for transplantation.....	63
Figure 17. AM-derived hepatic progenitor cells were successfully transplanted into an acute liver failure mouse model.....	66
Figure 18. The effect of AM-derived hepatic progenitor cells transplantation and efficiency.....	67
Figure 19. Schematic summary of in vivo study.....	68

## List of Tables

Table 1. Summary of characteristics of human mesenchymal stem cells from various tissues.....	27
---	----

## Abbreviations

UCM-MSCs: Umbilical cord matrix-derived mesenchymal stem cells

BM-MSCs: Bone marrow-derived mesenchymal stem cells

LD-MSCs: Liver-derived mesenchymal stem cells

AM-MSCs: Amnion-derived mesenchymal stem cells

FSC-SSC: Forward and Side scatter

OCT4: Octamer-binding transcription factor 4

SOX2: Sex-determining region Y-box 2

TNF- $\alpha$ : Tumor necrosis factor-alpha

TGF $\beta$ : Transforming growth factor-beta

OCR: Oxygen consumption rate

Nico: Nicotinamide

hHGF: Human hepatocyte growth factor

FGF2: Fibroblast growth factor 2

5-aza: 5-azacytidine

Fa: Fasudil

Dexa: Dexamethasone

ITS: Insulin-transferrin-selenium

PHH: Primary human hepatocytes

OSM: Oncostatin M

ALB: Albumin

CPM: Carboxypeptidase M

AFP: Alpha-fetoprotein

HNF4A: Hepatocyte nuclear factor 4 alpha

CYP3A4: Cytochrome P450 3A4

GATA6: GATA Binding Protein 6

SOX17: SRY-Box Transcription Factor 17

GSK3: Glycogen Synthase Kinase 3

CHIR: CHIR99021

EGF: Epidermal growth factor

HNF1A: Hepatocyte nuclear factor 1 alpha

CYP1A2: Cytochrome P450 1A2

UGT1A6: UDP Glucuronosyltransferase Family 1 Member A6

MRP2: Multiple drug resistance-associated protein 2

ASGR1: Asialoglycoprotein receptor 1

AM-HLCs: AM-MSC-derived hepatocyte-like cells

TAA: Thioacetamide

CTX: cyclophosphamide monohydrate

HGB: Hemoglobin

RBC: Red blood cells

ALT: Alanine aminotransferase

AST-GOT: Aspartate aminotransferase

H&E stains: Hematoxylin & eosin stain

IHC: Immunohistochemistry

mtDNA: Mitochondrial DNA



# **Chapter I.**

## **General Introduction**

## **I-1. Abstract**

The liver plays a critical role in the human body, such as detoxification of drugs, the synthesis of proteins and hormones, and supporting glycogen and cholesterol metabolism. Since it is an important organ, many people die from liver failure. Liver replacement therapy is considered a gold standard for patients with liver failure. However, there are many limitations to receiving liver transplantation for clinical treatment. Recently, stem cell technology has advanced and provided more expandable sources of liver cells for regenerative medicine. Mesenchymal stem cells (MSCs) can be isolated from diverse tissues and have stem cell markers, low immunogenicity, and differentiation potential. Moreover, MSCs are known to secrete liver regeneration-related growth factors and can support liver regeneration. Based on these findings, MSCs obtained from various organs have recently been explored as a more acceptable source of hepatocyte-like cells, especially with their ability to differentiate towards hepatogenic lineages.

In this part, we introduce the liver, liver disease, stem cells, and mesenchymal stem cells for understanding the overall thesis. Moreover, we investigated cell size, pluripotency, immunomodulation, and mitochondria function in the four different organ-derived MSCs, bone marrow (BM)-MSCs, umbilical cord matrix (UCM)-MSCs, liver-derived (LD)-MSCs, and amniotic membrane (AM)-MSCs. In the results, AM-MSCs had a small cell size and worked better immunomodulation and mitochondria function than other MSC lines. The stem cells also expressed pluripotent-related genes. Moreover, they had mass-production potential that was helpful for cell therapy. Therefore, we chose the AM-MSCs which were relatively suitable for cell therapy and hepatic differentiation, and used the cells in further study.

**Key words:** Liver, Liver failure, Stem cells, Mesenchymal stem cells, Umbilical cord matrix, Bone marrow, liver-derived, Amniotic membrane

## **I-2. Research Background and Introduction**

### **I-2-1. The Liver**

The liver is an organ of the digestive system only found invertebrates which are located in the right upper quadrant of the abdomen, below the diaphragm in humans [1, 2]. This organ plays a key role in the detoxification of drugs, the synthesis of proteins, and the production of biochemicals that are necessary for digestion and growth. Its also roles in metabolism include the production of hormones, the regulation of glycogen storage, and decomposition of red blood cells [3].

Cellular anatomically, the liver is composed of several cell types, such as hepatocytes, biliary epithelial cells (cholangiocytes), stellate cells, Kupffer cells, and liver sinusoidal endothelial cells. Each of these cells has unique functions that cooperatively regulate hepatic function [4]. Hepatocytes are the primary epithelial cell population of the liver. They comprise most of the liver volume, approximately 80 %, and perform many of the functions ascribed to the liver, such as protein synthesis, carbohydrate metabolism, lipid metabolism, and detoxification [5]. The proteins, which were synthesized by hepatocytes such as  $\alpha$ -fetoprotein, albumin, transferrin, plasminogen, fibrinogen, and clotting factors, were secreted into circulation. Particularly, serum albumin, synthesized only by hepatocytes, is the most abundant circulating protein and plays a critical role. It maintains the osmotic pressure of the blood compartment, provides nourishment of the tissues, and transports hormones, vitamins, drugs, and other substances such as calcium [6-8]. Moreover, the liver is the first organ exposed to venous blood draining from the gut. The venous blood, it composes of various toxins such as lipids and iron. Therefore, the liver should remove and process toxins that could damage organs without detoxification capabilities [9]. Cytochrome P450 (CYPs), which is located in the endoplasmic reticulum of hepatocytes, metabolizes various endogenous and exogenous chemicals and is important for the clearance of various compounds, such as toxins and drugs [10]. Thus, since the liver plays a critical role in the human body, liver failure from any number of sources is still a global problem

### **I-2-2. Liver Disease**

Liver disease can be the result of acute or chronic or acute-on-chronic causes such as alcohol, toxic drugs, viral infection, and genetic factors [11, 12]. There are four stages of the progress of liver disease; steatosis, fibrosis, cirrhosis, and end-stage liver disease (ESLD) [13]. In the early stage of the disease, as known as the steatosis stage, the liver becomes enlarged or inflamed with no symptoms. In this stage, the organ can be reversibly regenerated to normal liver. However, the inflammation continues, the damage can occur in liver fibrosis. Hepatic fibrosis is occurred by the wound-healing response of the

liver to repeated injury [14]. After occurring the inflammation injury, the organ starts to regenerate and replace the necrotic or apoptotic cells. However, since the regeneration capacity is limited, hepatocytes are substituted with abundant extracellular matrix (ECM), including fibrillar collagen. In this stage, the liver can be still reversibly regenerated, but treatment is needed [15]. After a long period of inflammation and fibrosis, a fibrotic liver advance to the cirrhosis stage. In this stage, the organ is impaired in its function. It is most commonly caused by alcoholic liver disease, non-alcoholic steatohepatitis, chronic hepatitis B, and chronic hepatitis C. The damage from cirrhosis generally cannot be reversed, but treatment, such as liver transplantation and palliative care, can stop or delay further progression [16]. Finally, continually advancing the liver cirrhosis, the organ is completely deteriorated and occurred the ESLD and liver cancer. In this stage, removal or transplantation of the normal liver is the only method to cure the organ.

Approximately 100,000 individuals per year are diagnosed with alcoholic liver disease and 12,000 people die only in the US [17]. Particularly, liver replacement or liver transplantation is considered the only cure method for patients with end-stage liver failure [18]. However, the shortage of available organs, high cost, the side effect of graft, and the requirement of lifelong immunosuppression, which can be occurred the incidence of tumor formation [19], makes it mandatory to seek alternate hepatic regeneration approaches. Recently, advanced stem cell technologies have extended the resources of regenerative medicine, and stem cells are expected to replace liver transplantation in the foreseeable future [20].

### **I-2-3. Stem cells**

Stem cells are defined that cells that have the ability of self-renewal and developmental potency. It can be differentiated into any type of cells followed by several specialization steps [21]. There are several types of stem cells, such as totipotent stem cells (TSC), pluripotent stem cells (PSC), induced pluripotent stem cells (iPSC), and mesenchymal stem cells (MSC). The TSC can differentiate into any type, such as the whole organism include the placenta, of cells. The example of TSC is a zygote. The PSC can form cells of all germ layers except extraembryonic structures like the placenta. Embryonic stem cells (ESC) are an example. The iPSC is multipotent stem cells that are generated from normal tissue cells using direct reprogramming technologies invented by Yamanaka Shinya [22, 23]. The discovery of these stem cells raises expectations for the treatment of diseases which cannot be cured by the present medical statement.

To obtain transplant cells for liver disease, hepatocytes or hepatic progenitor cells [24], PSC,

such as iPSC [25] or ESC [26], MSC [27], hepatic progenitor cells isolated from the liver or derived from hepatocytes, or hepatocytes themselves, are used [28]. Until now, these sources have had several limitations for clinical application. For example, iPSCs display a high risk of tumorigenicity and have low-efficiency differentiation ability, the use of ESCs is limited by their genetic background in terms of HLA types. However, unlike the cells described above, MSC can be easily extract from specific tissue in the human, such as bone marrow, umbilical cord blood, and grow readily in the culture dish. Moreover, they have intrinsic differentiation potentials and produce an abundance of useful growth factors and cytokines. MSCs have safety profiles to be used for clinical trials, these days. Thus, MSCs have been considerably expected as effective tools for cell-based therapy [29].

#### **I-2-4. Mesenchymal stem cells**

MSC are hierarchical postnatal stem cells that have a self-renewing and multi-lineages differentiation potency [30]. MSCs turn out to be a prominent issue in the research of stem cells area because of their biological significance and clinical applications. MSC has distinctive properties, such as ease of isolation and cultivation, plasticity, homing effect towards the injured area. They also perform the anti-inflammatory and anti-apoptotic activity in threatened tissues as well as immunomodulation, antimicrobial, and bacterial clearance activity [31]. These specific characteristics of MSC make an appropriate resource for the clinical treatment of diverse human diseases. Over the past 30 years, MSCs have exhibited an excellent safety profile for clinical trials, so that there are now over 950 registered MSC clinical trials listed with the Food and Drug Administration (FDA) [32].

Because of these properties, recently, MSC is used for differentiation studies, such as cardiomyocytes, neural, vascular, and liver. For cell therapy, primary tissue-derived cells extracted from the human organ are culture *in vitro* environment, but the culture is very difficult and makes them lose their own properties [33]. Thus, various research is conducted to obtain a large number of differentiated cells from MSC which is capable of mass robust culture for cell therapy [34].

In this study, we examined the characteristics of MSC extracted from bone marrow (BM), umbilical cord matrix (UCM), liver-derived (LD), amniotic membrane (AM). Then, we chose an appropriate MSC line for cell therapy using several parameters. Moreover, we established an efficient protocol using RNAseq analysis for differentiating AM-MSCs into HLCs by adding the GSK3 inhibitor, CHIR99021, and polyvinyl alcohol (PVA) instead of fetal bovine serum. We also conducted the hepatic function test of differentiated cells. Finally, we identified the optimum time for transplantation after initiating *in vitro* differentiation by measuring the expression of the carboxypeptidase M (*CPM*) and the

oxygen consumption rate of mitochondria. Hepatic progenitor cells transplanted into a mouse model induced by thioacetamide (TAA) and cyclophosphamide monohydrate (CTX) settled and cured in the damaged livers.

## **I-3. Materials and Methods**

### **I-3-1. Cell Isolation**

Mesenchymal stem cells were extracted from the liver tissue and amniotic membrane after delivery. The tissues were approved by the Institutional Review Board (IRB) of Asan Medical Center (Seoul, Korea; authorization number – liver tissue: 2018-1386; amniotic membrane: 2015-0303), and informed consent was obtained from participants.

To isolate the stem cells from each tissue, both were transferred into a Petri dish with 0.1 % collagenase IV and cut into small pieces under sterile conditions using operating scissors. The small pieces of tissue were transferred to a MACS C tube (Miltenyi Biotec, Bergisch Gladbach, Germany) and mechanically dissociated with a MACS Dissociator (Miltenyi Biotec). The dissociation method was followed by the manufacturer's instructions. After dissociating the tissues, dissociated cells were centrifuged at 500 x g for 3 min. The supernatant was removed, and RBC was lysed with 1 x RBC lysis buffer (eBioscience, San Diego, California, USA). Then, the culture medium was added and centrifuged at 800 x g for 3 min. The supernatant was removed, and the pellet was resuspended with a culture medium. The cells were plated in 0.1 % gelatin (Sigma Aldrich, MO, USA)-coated culture dishes. Only cell preparations with fibroblast-like morphology were used in further experiments.

### **I-3-2. Cell Culture**

In this study, human umbilical cord matrix and bone marrow-derived stem cells (UCM-MSCs and BM-MSCs) were provided by the Asan Stem Cell Center (Asan Institute for Life Sciences, Seoul, Korea). The cells were obtained from the previously described protocols [35]. All stem cells, such as UCM-MSCs, BM-MSCs, LD-MSCs, and AM-MSCs, were cultured on 0.1 % gelatin-coated culture dishes with a culture medium. The culture medium was composed of DMEM/F12 supplemented with 10% fetal bovine serum (FBS; Gibco, NY, USA), 10 ng/ml fibroblast growth factor 2 (FGF2; Peprotech, Rocky Hill, NJ, USA), 1% NEAA (Gibco), 1% Penicillin/Streptomycin (GeneDirex). The cells were passaged every 3 to 4 days using trypsin/EDTA (Gibco, NY, USA).

### **I-3-3. Cell surface proteins analysis**

Cell membrane surface proteins were measured by a flow cytometric machine. To analyze the stem cells, the stem cells were collected after detachment with trypsin/EDTA and stained for 30 min at 4°C with immunofluorescence-conjugated primary antibodies. The following antibodies were used in this study: PE-CD34, FITC-CD90, FITC-CD105, and FITC-CD47 (BD Biosciences Pharmingen, San

Diego, CA, USA). After staining, the cells were washed with PBS and suspended in 0.2 ml PBS for analysis. The fluorescence of samples was measured using a FACS Calibur (Becton Dickinson and Company, NJ, USA) and analyzed with FlowJo software (ver 10.6.1; Treestar, OR, USA).

#### I-3-4. Quantitative RT-qPCR

To measure a relative mRNA expression in four different types of mesenchymal stem cells, total RNA was extracted using an RNeasy Mini Kit (Qiagen, CA, USA) following the manufacturer's instructions. Then, cDNA was synthesized using an Ultrascript 2.0 cDNA Synthesis Kit (PCR Biosystems, London, UK), and qRT-PCR was conducted with a Power SYBR® Green PCR Master Mix (Applied Biosystems, CA, USA) on a QuantStudio™ real-time PCR System (Applied Biosystems). *GAPDH* was used as an internal control. The primer sequences, which were used in this study, are listed below the table.

Gene name	Primer sequence (5' to 3')	*F, Forward; R, Reverse
<i>OCT4</i>	F: GAAGGATGTGGTCCGAGTGT R: GTGAAGTGAGGGCTCCCAT	
<i>NANOG</i>	F: CAAAGGCAAACAACCCACTT R: TCTGCTGGAGGCTGAGGTAT	
<i>SOX2</i>	F: AACCCCAAGATGCACAACCTC R: CGGGGCCGGTATTTATAATC	
<i>TNF<math>\alpha</math></i>	F: TCAGATCATCTTCTCGAACCCC R: ATCTCTCAGCTCCACGCCAT	
<i>IL-1<math>\beta</math></i>	F: AATCTGTACCTGTCCTGCGTGTT R: TGGGTAATTTTTGGGATCTAACTCT	
<i>IL-6</i>	F: GGAGACTTGCCTGGTGAAAA R: GTCAGGGGTGGTTATTGCAT	
<i>TGF<math>\beta</math>1</i>	F: GGCCAGATCCTGTCCAAGC R: GTGGGTTTCCACCATTAGAC	
<i>IL-10</i>	F: GGTGCCAAGCCTTGTCTGA R: AGGGAGTTCACATGCGCCT	
<i>ALP</i>	F: ACCATTCCCACGTCTTCACATTT R: AGACATTCTCTCGTTCACCGCC	
<i>OCN</i>	F: CAAAGGTGCAGCCTTTGTGTC R: TCACAGTCCGGATTGAGCTCA	
<i>FABP4</i>	F: GCTTTGCCACCAGGAAAGTG R: ATGGACGCATTCCACCACCA	
<i>PPAR<math>\gamma</math></i>	F: GATACTGTCTGCAAACATATCACAA R: CCACGGAGCTGATCCCAA	
<i>GAPDH</i>	F: GCCTCAAGATCATCAGCAATGC R: TGGTCATGAGTCCTTCCACGAT	

#### I-3-5. Mixed Lymphocyte Reaction assay

To measure the immunomodulation of MSCs, we conducted a mixed lymphocyte reaction (MLR) assay which was previously reported [36]. Briefly, peripheral blood mononuclear cells (PBMCs) were isolated from 2 different healthy volunteers by density gradient centrifugation using Ficoll-Paque PLUS (GE



Healthcare, Piscataway, NJ, USA). One lot of PBMCs were treated with 10  $\mu\text{g/mL}$  mitomycin C (Sigma Aldrich, St. Louis, MO, USA) solution to prepare stimulated cells. After 1 h, the cells were washed with RPMI 1640 (Hyclone) supplemented with 10% FBS at least 3 times. MLR assays were performed by co-culturing PBMCs obtained from identical individuals or PBMCs from different individuals in 96-well flat-bottom plates (Corning Incorporated – Life Sciences, Durham, NC, USA) ( $1.0 \times 10^5$  cells/well), respectively. The cells were incubated at 37 °C with 5% CO<sub>2</sub> for 9 days. To measure the effect of stem cells on immune cell proliferation, UCM-MSCs, BM-MSCs, LD-MSCs, and AM-MSCs were passaged, counted, seeded, and co-cultured with PBMCs ( $1.0 \times 10^5$  cells/well) for 96 h. To measure the proliferation index, viable cells were counted using the Viability Assay Kit (MediFab, Seoul, South Korea) according to the manufacturer’s instructions. Briefly, cell viability solution was added to each well before adding stem cells and 96 h after co-culturing with stem cells. After a 2 h incubation, the optical density was measured at a wavelength of 450 nm. The proliferation index was calculated by dividing the mean optical density values of cultured cells after 96 h with the mean optical density value of cells before the addition of stem cells (n = 4).

#### **I-3-6. Seahorse assay**

To measure oxygen consumption rates (OCR), four different types of mesenchymal stem cells were seeded at 7000 cells/cm<sup>2</sup> in 0.1% gelatin-coated XF24 cell culture plates (Agilent Technologies, Santa Clara, CA, USA). Mitochondrial OCR was measured with an XF Cell MitoStress test kit in an XF24 extracellular flux analyzer (Agilent Technologies) and calculated as described [36]. Values were normalized by the amount of cellular DNA.

#### **I-3-7. Osteogenesis and adipogenesis of AM-MSCs**

Differentiation was performed using Osteogenesis and Adipogenesis differentiation Kit (Thermofisher Scientific) to generate the osteocytes and adipocytes in AM-MSCs. The differentiation protocols were performed according to the kit’s recommendations.

#### **I-3-8. Measuring the cell growth rate**

To measure the extent of cell growth rate, stem cells were seeded at  $1 \times 10^5$  cells in 0.1% gelatin-coated 6-well plates at every passage. Cell numbers were counted by hemocytometer. The extent of cell number was calculated as a cell growth rate from the formula: Day 3 cell number/ $1 \times 10^5$  cells.

### I-3-9. Production of B2M-KO-AM-MSCs

Human genomic B2M sequences were analyzed and selected using the web tool Benchling (<https://benchling.com/>). B2M-specific CRISPR-Cpf1 expression vector was constructed by cloning the annealed oligomers (5'-agatCCGATATTCCTCAGGTACTC-3' and 5'-aaaaGAGTACCTGAGGAATATCGG-3') into a pY108 lentiviral vector (Addgene, plasmid #84739). Infectious lentiviral particles were produced as described previously and were precipitated using Lenti Concentrator (Origene, Rockville, Maryland, US) according to the manufacturer's protocol [37]. To produce stable B2M-KO-AM-MSCs, resuspended lentivirus in culture media were added to AM-MSCs and were incubated for 24 h in the culture medium. The cell culture medium was replaced with a fresh medium containing 4 µg/ml puromycin and incubation continued for a further 24 h. AM-MSCs in which B2M was knocked out and that did not express MHC I was selected with a BD FACSAria™ III Cell Sorter. B2M-KO was accessed by an Indel sequencing primer like the below table.

Gene name	Primer sequence (5' to 3')	*F, Forward; R, Reverse
<i>B2M (Indel sequencing primer)</i>	F: GCTATGAGTGCTGAGAGGGC R: CACGGCAGGCATACTCATCT	

### I-3-10. Statistical analysis

All experiments were performed on at least three (n = 3) independent biological samples, and data are presented as means ± standard deviations (SD). Statistical analysis was performed using GraphPad Prism 6.0 software (GraphPad Software, CA, USA). Comparisons of three or more data sets were performed by one-way ANOVA followed by Bonferroni's multiple comparison tests. Two-group comparisons were made using two-tailed Student's t-tests. P <0.05 was considered statistically significant.

## **I-4. Results**

### **I-4-1. Phenotypical comparison of human mesenchymal stem cells from the umbilical cord, bone marrow, liver, and amniotic membrane**

To characterize four different types of mesenchymal stem cells (umbilical cord matrix-derived mesenchymal stem cells (UCM-MSCs), bone marrow-derived MSCs (BM-MSCs), liver-derived mesenchymal stem cells (LD-MSCs), and amniotic membrane-derived mesenchymal stem cells (AM-MSCs)), we compared a shape, CD marker, size, and pluripotent-related genes of the stem cells. Morphologically, the four different MSCs were fibroblast-like shapes with ovoid nuclei as known as common MSCs [38] (Figure. 1A). Moreover, all types of MSCs have expressed the MSC surface markers, CD90 and CD105, but did not express CD34 like common MSCs [39] (Figure. 1B). In terms of size and granularity, AM- and LD-MSCs were relatively smaller than other types of MSC lines, while the BM-MSCs were relatively biggest (Figure. 1C). All types of MSCs were expressed pluripotent genes, such as *OCT4*, *NANOG*, and *SOX2*. *OCT4* was most expressed in AM-MSCs, while *NANOG* and *SOX2* were most expressed in BM-MSCs (Figure. 1D).

### **I-4-2. Cellular characteristics as human mesenchymal stem cells**

We also researched about cellular characteristics of four MSC lines. Previous studies have reported that MSCs were expressed various inflammation-related cytokines, and modulated immune systems [32]. Therefore, we measured the expression of anti- and pro-inflammation-related cytokines in four different types of MSC lines. As we expected, the inflammation-related cytokines were expressed in four types of MSCs, but the expression levels were all different (Figure. 2A). Next, we evaluated the immunomodulation of four different types of MSCs using a mixed lymphocyte assay. As a result, AM-MSCs and LD-MSCs had relatively higher immunomodulation capacity than other MSCs lines (Figure. 2B). We also measured the mitochondrial function of stem cells using seahorse assay in three other MSCs, such as UCM-MSCs, LD-MSCs, and AM-MSCs. Previous studies have reported that mitochondria play an important role in regulating stem cell activity and fate decisions. Low mitochondrial function in stem cells induced deterioration of stem cell function [40]. Therefore, we evaluated the mitochondrial function in stem cells to select appropriate stem cells for use in hepatic differentiation. As a result, maximal OCR levels were significantly high in AM-MSCs, and ATP production was significantly high in two different AM-MSC lines (Figure. 2D).

Finally, we summarized the characteristics of four other MSC lines and chose the MSC lines to be suitable for cell therapy and hepatic differentiation based on the summary (Table. 1). We evaluated

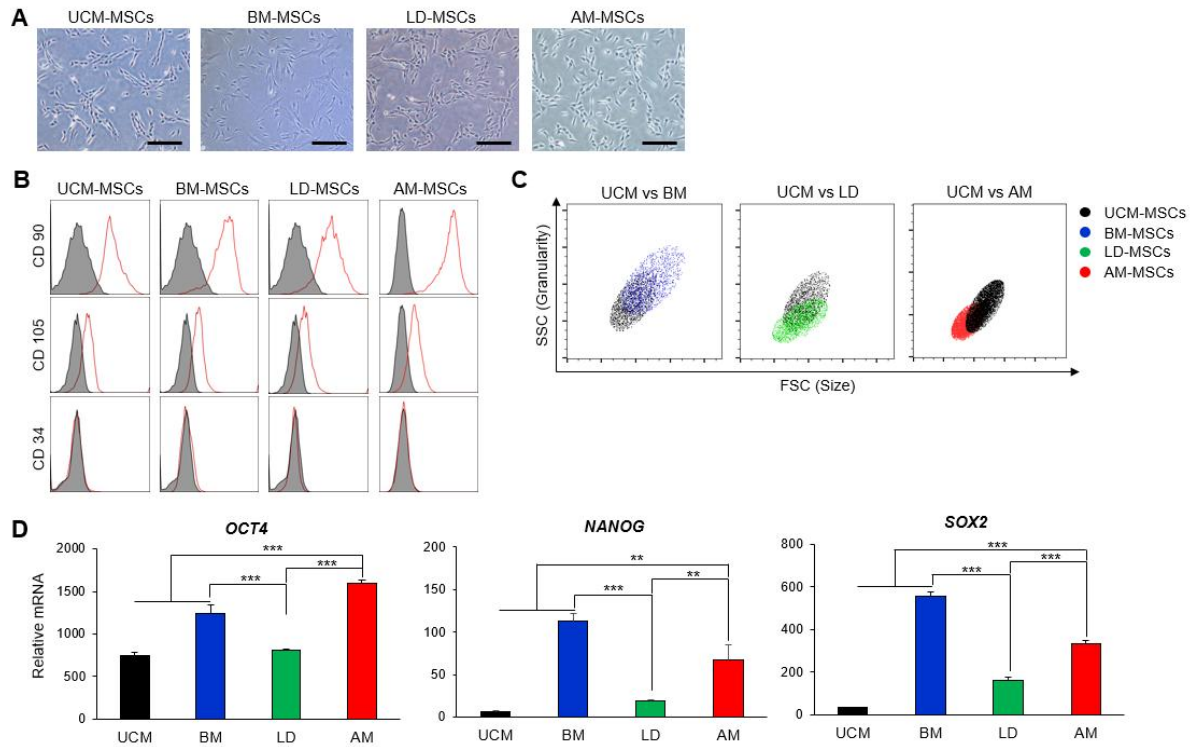


**Figure 1. The phenotypes of human mesenchymal stem cells from various tissues.**

(A) Morphology of mesenchymal stem cells (MSCs) isolated from the various organ, umbilical cord matrix (UCM), bone marrow (BM), liver (LD), amniotic membrane (AM). Scale bar = 200  $\mu$ m. (B) Flow cytometric analysis shows that all MSCs had similar characteristics in terms of expression of MSC surface markers (CD90 and CD105) and absence of a hematopoietic stem cell marker (CD34). (C) The relative comparison of cell size using flow cytometric graph, FSC-SSC plot. FSC represents cell size, and SSC represents the granularity of cells in flow cytometry (Black dot: UCM-MSCs, Blue dot: BM-MSCs, Green dot: LD-MSCs, Red dot: AM-MSCs). (D) RT-qPCR analysis of pluripotency-related genes, *OCT4*, *NANOG*, and *SOX2*. *GAPDH* was used as an internal control. P-values < 0.05 were considered significant. \*, P < 0.05; \*\*, P < 0.01, \*\*\*, P < 0.001.

the stem cells under four other characteristics, such as cell size, pluripotency, immunomodulation, and mitochondrial function. The cell size of MSCs is significantly bigger when they are injected into the vascular [41]. Moreover, pluripotency and mitochondrial function were important characteristics for differentiation, and immunomodulation was critical for transplantation [42]. Thus, when evaluated from four characteristics, AM-MSCs were the most suitable MSC line for cell therapy and hepatic differentiation. AM-MSCs had lower pluripotency than BM-MSCs, but it has advantages of size, immunomodulation, and mitochondrial function.

### **I-4-3. The mass-production potential of AM-MSCs**

For applications as cell-based therapies, large-scale expansion of stem cells is required. To test the mass-production potential of AM-MSCs, we counted the number of stem cells isolated per cm<sup>2</sup> of the amniotic membrane (Figure. 3A). In three independent experiments, the average number of AM-MSCs has harvested 2 x 10<sup>6</sup> cells per cm<sup>2</sup>. These stem cells were grown at least 8-fold at every passage up to 10-passage (Figure. 3B).

To confirm that AM-MSCs maintain their characteristics until passage 10, first, we measured the mRNA expression of pluripotent markers [43], *OCT4*, *NANOG*, and *SOX2*, in every other passage. All three genes were expressed at similar levels among passages (Figure. 3C). Second, we examined the mesenchymal lineage differentiation ability and conducted osteogenic and adipogenic differentiation using passages 2 and 10 of AM-MSCs. Both passages were highly expressed than undifferentiated AM-MSCs in terms of the osteogenic markers; *ALP* and *OCN* and adipogenic markers; *PPAR $\gamma$*  and *FABP4* ( $P < 0.001$ , Figure. 3D). Between 2 passages, the levels were comparable, suggesting that AM-MSCs maintained their differentiation ability at passage 10.

In conclusion, since the stem cells have shown a growth more than 5 times per passage up to passage 10 while maintaining stemness, more than 10<sup>13</sup> cells could be obtained from a donor individual (Figure. 4). Given that a maximum of 2 x 10<sup>8</sup> cells is used per person in clinical trials of transplantation [44], this yield would be sufficient to treat more than 10,000 individuals. Moreover, because of the characters that large-scale culture is possible, hepatocytes can be produced through hepatic differentiation of AM-MSCs in large quantities to treat liver disease.

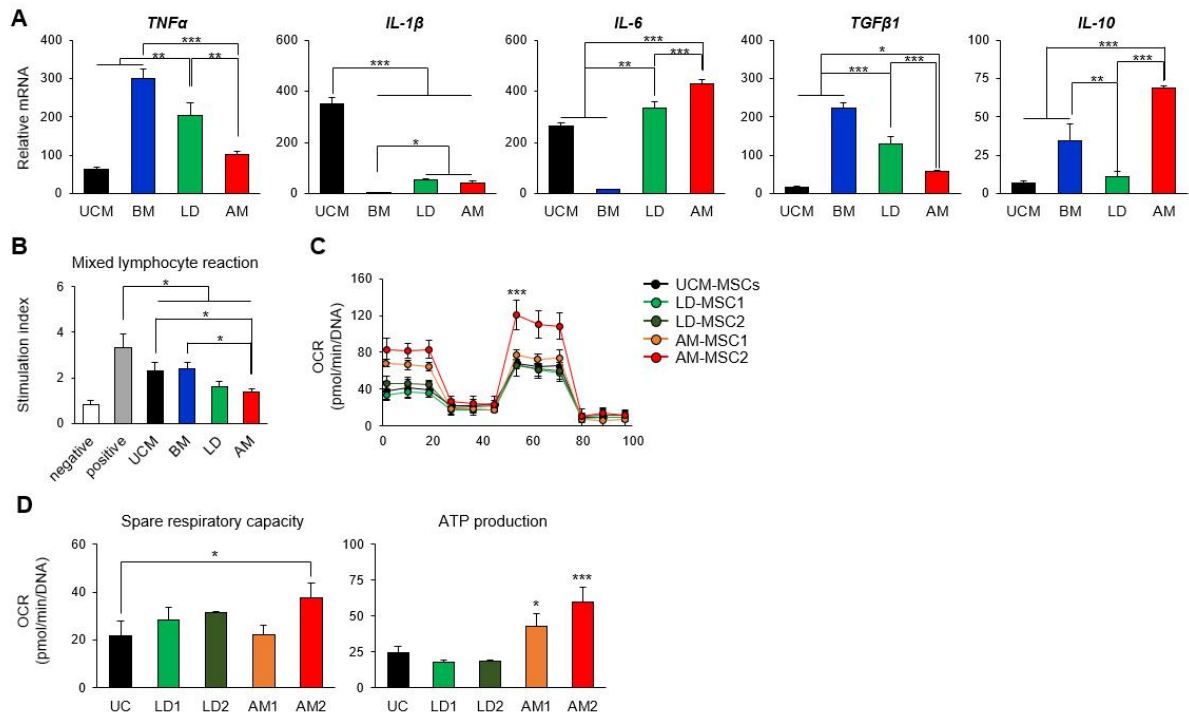


**Figure 2. Cellular characteristics of human mesenchymal stem cells.**

(A) RT-qPCR analysis of inflammatory-related genes, *TNF- $\alpha$* , *IL-1 $\beta$* , *IL-6*, *TGF $\beta$ 1*, and *IL-10*. *GAPDH* was used as an internal control. (B) The evaluation of PBMC immune response with MSCs. All control groups were only cultured in a medium without MSC. Negative control: PBMC cultured with the single donor, Positive control: PBMC cultured with another donor. (C) Seahorse assay of four other MSCs, such as UCM-MSCs, LD-MSCs, and AM-MSCs. (D) Oxygen consumption rates (OCR) values of spare respiratory capacity and ATP production. OCR values were normalized by the DNA concentration. P-values < 0.05 were considered significant. \*, P < 0.05; \*\*, P < 0.01, \*\*\*, P < 0.001.

	UCM	BM	LD	AM
size	average	big	small	small
Pluripotency	+	+++	+	++
Immunomodulation	+	+	++	++
Mitochondria function	+	n.e	+	+++

\* Not experimented

**Table 1. Summary of characteristics of human mesenchymal stem cells from the various organ.**

The summary table of four other MSC's characteristics. The size was measured in Figure 1C using flow cytometry. The pluripotency was scored that based on Figure 1D. The immunomodulation was scored that based on Figure 2B. The mitochondria function was scored that based on Figures 2C and D.

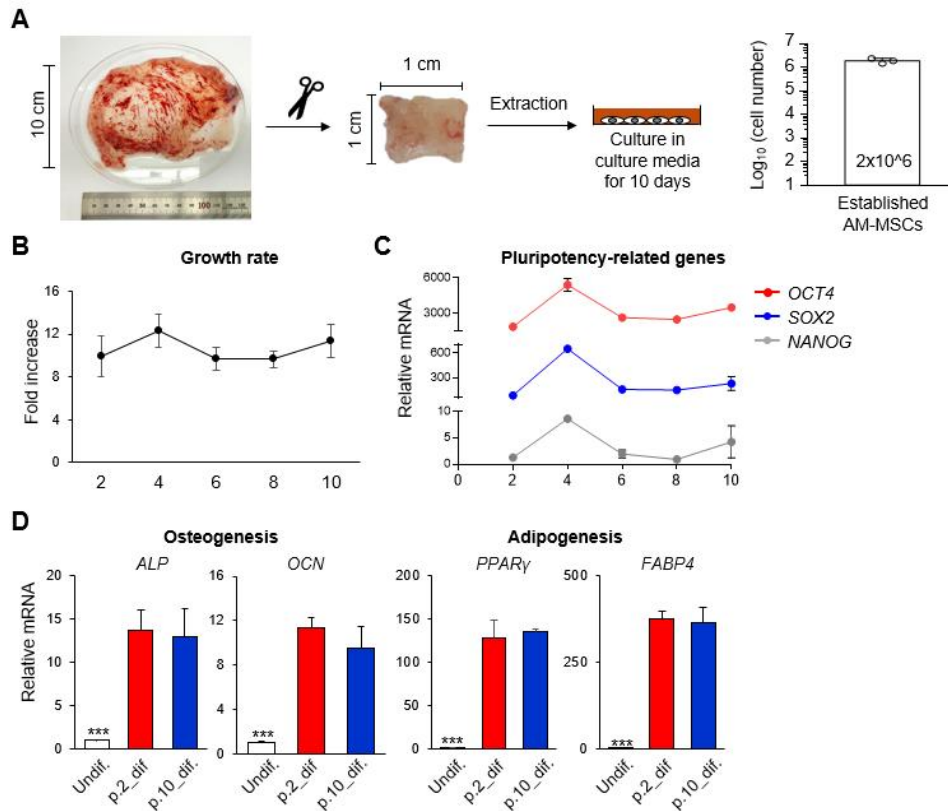


**Figure 3. Mass production of AM-MSCs.**

(A) The isolation procedure, and the number of established AM-MSCs per cm<sup>2</sup> of the amniotic membrane. Y-axis values represent the logarithm of total cell numbers. (B) The growth rate of AM-MSCs is based on passages (Biological replication, n = 3). (C) mRNA levels of pluripotency-related genes *OCT4*, *SOX2*, and *NANOG* according to the passage number (Technical replication, n = 3). (D) mRNA expression analysis of osteogenesis-related (*ALP*, *OCN*) and adipogenesis-related (*PPAR $\gamma$* , *FABP4*) genes on AM-MSCs and day 14 after the induction of differentiation using early (p.2) and late (p.10) passage of AM-MSCs. *GAPDH* was used as an internal control for RT-qPCR. P-values < 0.05 were considered significant. \*, P < 0.05; \*\*, P < 0.01, \*\*\*, P < 0.001.



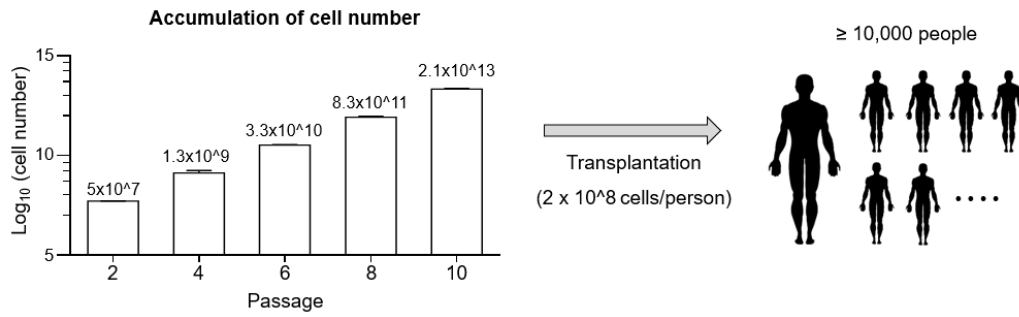


**Figure 4. Estimation of total cell numbers during the passage.**

More than  $2 \times 10^{13}$  AM-MSCs could be harvested after ten passages. If maximally, the  $2 \times 10^8$  cells are used to transplant into a patient, it can be used in more than 10,000 people. Y-axis values represent the logarithm of total cell numbers.

#### **I-4-4. Generation of universal cells from AM-MSCs**

We also induced B2M-knocking out on AM-MSCs to show potential as universal donors. To generate B2M-KO-MSCs, we targeted the B2M gene, which up-regulates MHC I, using the CRISPR-Cpf1 system (Figure. 5A) [45]. Stem cells, including AM-MSCs, are MHC I positive, and so can cause immune rejection in transplanted recipients. After inducing B2M-knockout (KO), MHC I-negative cells were sorted by flow cytometry. As we expected, the expression of MHC I was declined, and the B2M gene was successfully knockout (Figure. 5B and C). The KO-AM-MSCs have measured the expression of MSC CD markers. The CD90 and CD105 expressed positively while CD34 was negative (Figure. 6A), but the growth rate was decreased in the B2M-KO (Figure. 6B). However, interestingly, CD47 expression was up-regulated than intact AM-MSCs (Figure. 6C). The CD47 protects transplanted cells from macrophage phagocytosis. This is because when CD47 expression is low, macrophages can recognize the transplanted cells as non-self, known as the do not eat me signal [46]. Finally, we evaluated the immune response of B2M-KO-AM-MSCs with human PBMCs using a proliferation assay. The B2M-KO-AM-MSCs were comparable proliferation with negative control while significantly lower than intact AM-MSCs ( $P < 0.05$ , Figure. 6D) suggesting less immune response.

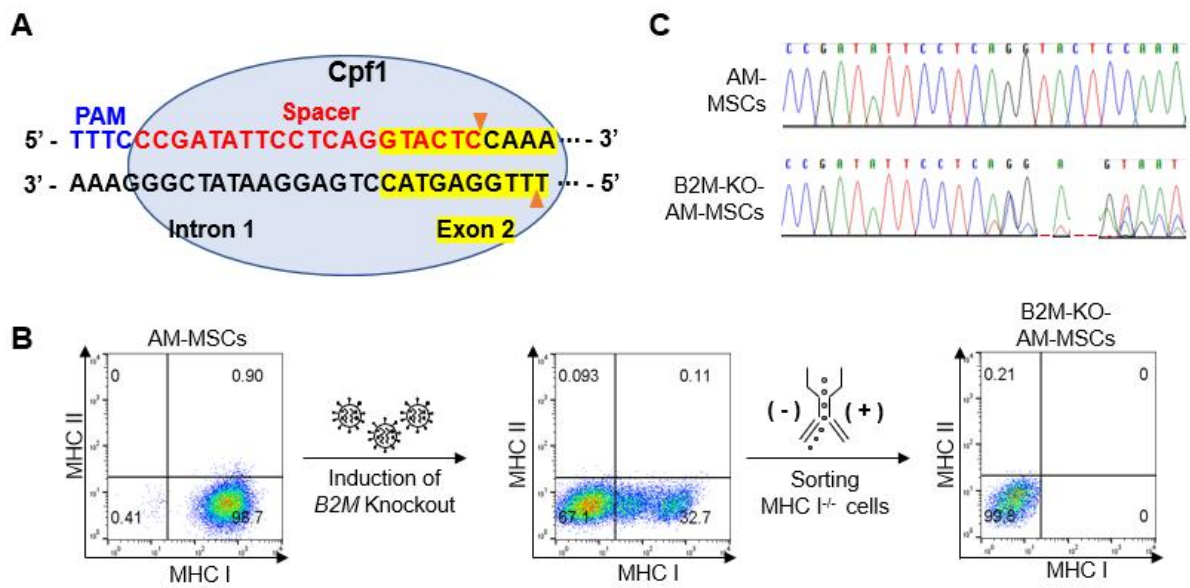


**Figure 5. Generation of hypo-immune potential universal cells from AM-MSCs.**

(A) The target DNA sequence in the human B2M locus is shown in red. (B) Scheme of the process for generating universal donor AM-MSCs. After inducing B2M knockout, MHC I-negative AM-MSCs are selected by flow cytometry. (C) Sequencing of B2M in MHC I-KO and AM-MSCs after B2M knockout in AM-MSCs.

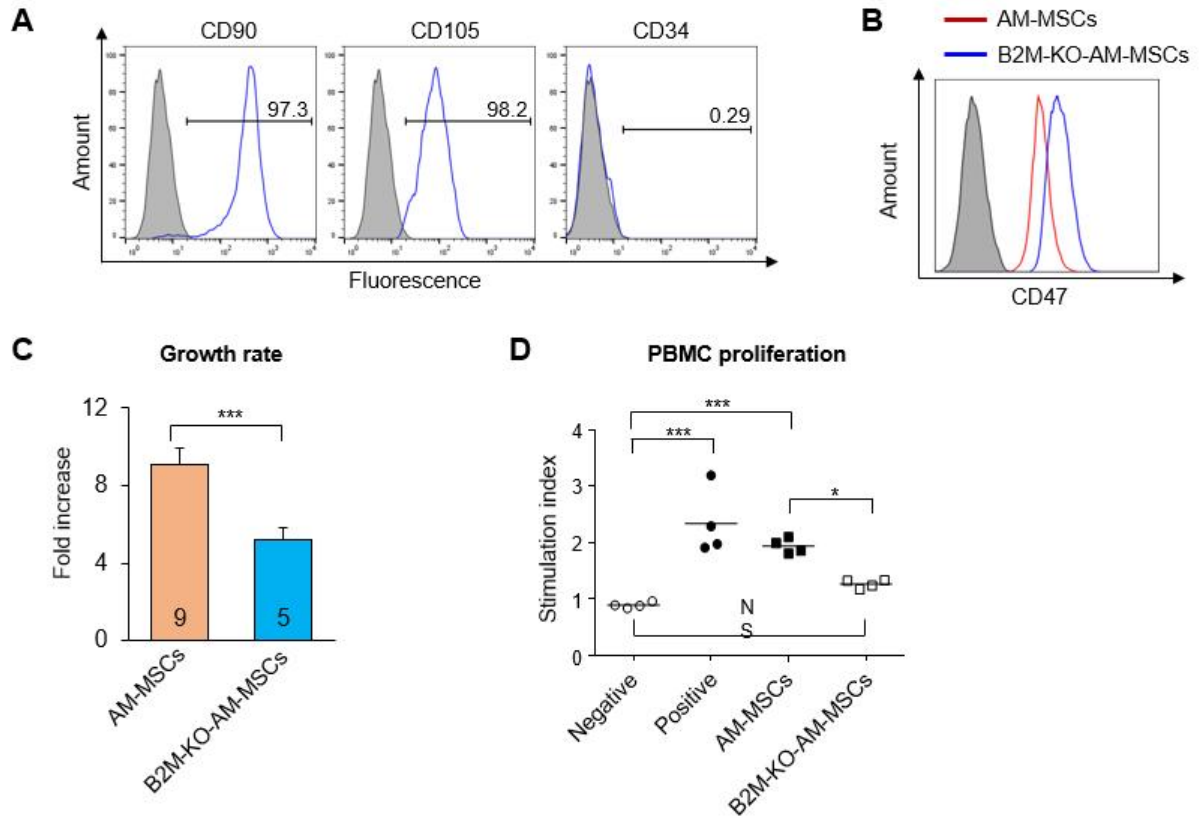


**Figure 6. Phenotypes of hypo-immune potential universal cells from AM-MSCs.**

(A) Expression of MSC CD markers (CD90, CD105) and hematopoietic markers (CD34) in B2M KO-AM-MSCs. (B) CD47 expression levels in AM-MSCs and B2M-KO AM-MSCs analyzed by flow cytometry. (C) Growth rate of AM-MSCs and B2M-KO-AM-MSCs. B2M-KO: B2M-KO-AM-MSCs. (D) The evaluation of PBMC proliferation assays (4 donors of PBMCs). All control groups were only cultured in a medium without MSC. Negative control: PBMC cultured without PHA, Positive control: PBMC cultured with PHA. P-values < 0.05 were considered significant; \*, P<0.05; \*\*, P<0.01; \*\*\*, P<0.001.

**Chapter II.**  
**The study of**  
***in vitro* hepatic differentiation**

## II-1. Abstract

Amniotic membrane-derived mesenchymal stem cells (AM-MSCs) are an attractive source of stem cell therapy for patients with irreversible liver disease. However, there are obstacles to their use because of low efficiency and xeno-contamination for hepatic differentiation.

In this part, we established an efficient protocol for differentiating AM-MSCs into hepatocyte-like cells (HLCs) by comparing transcriptomes data between AM-MSCs and UC-MSCs. In AM-MSCs, *GATA6*, *EGF*, *AFP*, and *FGF2* were downregulated, while *GSK3* was upregulated. The gene expression profiles of the cells were not familiar with hepatic differentiation. Based on this result, we established an efficient hepatic differentiation protocol using the GSK3 inhibitor, CHIR99021, and enhance the efficiency of differentiation. Furthermore, to generate the xeno-free conditioned protocol, we altered fetal bovine serum (FBS) to polyvinyl alcohol (PVA). Replacing FBS with PVA resulted in improved differentiation ability, such as upregulation of hepatic maturation markers. Finally, we investigated the hepatocyte functions. The differentiated hepatocyte-like cells (HLCs) not only synthesized and secreted albumin but also metabolized drugs by the CYP3A4 enzyme.

**Key words:** AM-MSCs, UC-MSCs, in vitro hepatic differentiation, transcriptome analysis, CHIR99021, FBS, PVA, Xeno-free, hepatic function

## II-2. Introduction

In embryogenesis, the liver is developed in both the ventral portion of the foregut endoderm and the constituents of the adjacent septum transversum mesenchyme [47]. The mesenchyme of the septum transversum induces the tube of endoderm, which is known as hepatic diverticulum and origin of the liver, to proliferate, and to make the glandular epithelium of the liver. Continuously signaling from the septum transversum mesenchyme, both fibroblast growth factor (FGF) from the developing heart and retinoic acid from the lateral plate mesoderm also contributes to forming the hepatic endodermal cells. The hepatic endodermal cells transform from columnar to pseudostratified resulting in thickening into the early liver bud. Their transformation subsequently forms a population of the bipotential hepatoblasts, as known as hepatic progenitors. The hepatic progenitors differentiate into biliary epithelial cells (cholangiocytes) and hepatocytes which are largely populated in the liver [48]. The study on liver development influences the hepatic differentiation of stem cells and enhances the stem cell technologies level.

To successfully induce hepatocytes, induction of endoderm is a critical step. As described above, the liver is derived from the definitive endoderm in the development, and transforming growth factor  $\beta$  (TGF  $\beta$ ) superfamily signaling is necessary for endoderm specification. Especially, WNT and FGF are required for the normal formation of the primitive streak and the induction of the key endoderm marker, SOX17 [49]. However, in the *in vitro* differentiation, because it is difficult to completely handle these signals, the endoderm induction results in poor efficiency. Therefore, most protocols of endoderm differentiation modulate the signal pathway either by the addition of recombinant WNT protein or by inhibition of GSK3 and PI3K using small molecules or by removing insulin [50]. After inducing the endoderm, for further maturation, hepatocyte growth factor (HGF), oncostatin M (OSM), and dexamethasone (Dexa) are needed. OSM and Dexa play an important role in liver maturation from developing hepatocytes. OSM has downregulated the SOX family and advanced the differentiation of hepatocytes from endoderm and hepatoblasts [51]. Dexa induces the expression of both HNF4 and C/EBP-alpha which are crucial for differentiation for hepatocytes. [52]. In these processes, hepatocyte-like cells (HLC) can be induced from the stem cells.

Human amniotic membranes (AM) are high-yielding sources of stem cells [53]. Moreover, followed by the studies of part I, AM-MSCs were a good source for the studies of differentiation and cell therapy. However, there are some obstacles to successfully differentiating the AM-MSCs into HLC for therapeutic uses. FBS is a highly effective growth supplement for cell culture and many studies of differentiation. However, there is batch-to-batch variability that may affect cell characteristics, and the

risk of contamination with harmful pathogens in human transplantation studies [54, 55]. Accordingly, progressive attempts have been made to devise chemically defined xeno-free culture conditions for stem cells [56, 57]. Moreover, since stem cells have different gene expressions according to their origin, the differentiation methods should be slightly different.

Thus, in the part II studies, we analyzed the transcriptomes of several stem cells and established an efficient protocol for hepatic differentiation of AM-MSCs and altered fetal bovine serum (FBS) to polyvinyl alcohol (PVA).



## II-3. Materials and Methods

### II-3-1. Quantitative RT-qPCR

To measure a relative mRNA expression in the hepatic differentiated cells, total RNA was extracted using an RNeasy Mini Kit (Qiagen, CA, USA) following the manufacturer's instructions. Then, cDNA was synthesized using an Ultrascript 2.0 cDNA Synthesis Kit (PCR Biosystems, London, UK), and qRT-PCR was conducted with a Power SYBR® Green PCR Master Mix (Applied Biosystems, CA, USA) on a QuantStudio™ real-time PCR System (Applied Biosystems). *GAPDH* was used as an internal control. The primer sequences, which were used in this study, are listed below the table.

Gene name	Primer sequence (5' to 3')	*F, Forward; R, Reverse
<i>CPM</i>	F: GGATGGAAGCGTTTTGAAG R: CCACAACAAGAACCCACAGG	
<i>AFP</i>	F: AGACTGCTGCAGCCAAAGTGA R: GTGGGATCGATGCTGGAGTG	
<i>ALB</i>	F: TGCTGATGAGTCAGCTGAAAA R: TCAGCCATTTACCATAGGTT	
<i>HNF4A</i>	F: CAGGCTCAAGAAATGCTTCC R: GGCTGCTGTCCTCATAGCTT	
<i>CYP3A4</i>	F: TTTTGTCTACCATAAGGGCTTT R: CACAGGCTGTTGACCATCAT	
<i>GATA6</i>	F: GAGGCTTGCTGAAAGAGTGAGAGAAGA R: TCCTAGTCCTGGCTTCTGGAAGTG	
<i>SOX17</i>	F: CAAGGGCGAGTCCCGTAT R: CGACTTGCCCAGCATCTT	
<i>UGT1A6</i>	F: GCCCTGTGATTTGGAGAGTGA R: AGGCTTCAAATTCCTGAGACAAGT	
<i>CYP1A2</i>	F: CGGACAGCACTTCCCTGAGA R: AGGCAGGTAGCGAAGGATGG	
<i>MRP2</i>	F: AGCGTCCTCTGACACTCG R: GGCATCTTGGCTTTGACT	
<i>ASGR1</i>	F: CAGCAACTTCACAGCCAGCA R: AGCTGGGACTCTAGCGACTT	
<i>HNF1A</i>	F: TGGGTCCTACGTTACCAAC R: TCTGCACAGGTGGCATGAGC	
<i>GAPDH</i>	F: GCCTCAAGATCATCAGCAATGC R: TGGTCATGAGTCCTTCCACGAT	

### II-3-2. Seahorse assay

To measure oxygen consumption rates (OCR), the cells were seeded at 7000 cells/cm<sup>2</sup> in 0.1% gelatin-coated XFe24 cell culture plates (Agilent Technologies, Santa Clara, CA, USA). Especially, to measure the OCR of differentiated cells, stem cells were seeded in the plate and conducted the hepatic differentiation. Mitochondrial OCR was measured with an XF Cell MitoStress test kit in an XF24 extracellular flux analyzer (Agilent Technologies) and calculated as described [36]. Values were

normalized by the amount of cellular DNA.

### **II-3-3. Immunocytochemical staining**

Cells were fixed with 4% formaldehyde overnight, washed with the PBST buffer, permeabilized in 0.5% Triton X-100 and blocked in PBST with 1% bovine serum albumin (Sigma Aldrich). Samples were incubated with primary antibodies, anti-human Albumin, and anti-human CYP3A4 (1:100; Santa Cruz Biotechnology, Dallas, TX, USA) overnight at 4°C, followed by goat anti-mouse IgG Alexa Fluor 488-conjugated and donkey anti-rabbit IgG Alexa Fluor 488-conjugated secondary antibody (1:500; Abcam). Nuclei were counterstained with 4', 6-diamidino-2-phenylindole (DAPI) (Sigma Aldrich) for 10 min, and fluorescence signals were detected using an AxioObserver Z1 microscope (Carl Zeiss, Oberkochen, Germany).

### **II-3-4. Transcriptome analysis**

To compare the transcriptome between AM-MSCs (n = 3) and UCM-MSCs (n = 3), total RNA was extracted using an RNeasy Mini Kit (Qiagen) following the manufacturer's instructions. All cells were sequenced by strand-specific, paired-end sequencing (Illumina, San Diego, CA, USA), generating approximately 1.1 to 1.3 x 10<sup>6</sup> reads per sample. The quality of the raw data sets was analyzed with the software FastQC (v0.11.5), and adapter sequences of < 20 bp in length, and sequences with a quality score lower than Q20, were removed using Cutadapt software (v1.5) to increase mapping quality. After trimming, the remaining sequences, constituting 97.3 to 98.8% of the raw data sets, were aligned with the human reference genome (GRCh38.p13) using STAR software (v2.7.5c), and reads were summarized using featureCount software. Normalization of reads, analysis of gene expression, and calculation of differentially expressed genes was performed using DESeq2 (1.28.1). Gene Ontology Enrichment Analysis of the differentially expressed genes was conducted using online tools (<http://geneontology.org>). Functional enrichment in the Biological Process of the GO terms was analyzed. A list of hepatic-associated genes was retrieved from the online human gene database (<https://www.genecards.org/>).

### **II-3-5. *In vitro* hepatic differentiation**

Stem cells were differentiated by the previously published conventional hepatogenic differentiation protocol [36] and an advanced protocol. Briefly, in the advanced protocol, the cells were seeded on 0.1% gelatin-coated dishes at 7000 cells/cm<sup>2</sup> in a cell culture medium. After two days, they were cultured for

seven days with Step-1 medium consisting of Iscove's Modified Dulbecco's Medium (IMDM; Gibco) supplemented with 0.1% polyvinyl alcohol (PVA; Sigma Aldrich) or 1% FBS, 10 mM nicotinamide (Sigma Aldrich), 20 ng/ml hHGF (Peprotech), 10 ng/ml FGF2, 2  $\mu$ M 5-azacytidine (Sigma Aldrich), 0.1  $\mu$ M dexamethasone (Sigma Aldrich), 1% insulin-transferrin-selenium (ITS; Gibco), 3  $\mu$ M CHIR99021, 20 ng/ml EGF (Peprotech), and 10  $\mu$ M Fasudil (AduoQ Bioscience, Irvine, CA, USA). For hepatic maturation, the Step-1 medium was replaced with Step-2 medium consisting of IMDM supplemented with 1  $\mu$ M dexamethasone, 1% ITS, 20 ng/ml Oncostatin M (OSM, Peprotech), 20 ng/ml hHGF, and 10  $\mu$ M Fasudil.

### **II-3-6. Culture for primary human hepatocytes**

Primary human hepatocytes (PHH) were purchased from ThermoFisher Scientific (HMC PMS; ThermoFisher Scientific, MA, USA), and were cultured and maintained according to the supplemented protocol. In brief, the hepatocytes were thawed in Cryopreserved hepatocytes recovery medium (CM7000; ThermoFisher Scientific), centrifuged at 100 x g for 10 min, and seeded at  $2 \times 10^6$  cells/well on a collagen-coated plate in cryopreserved hepatocyte plating medium (CM9000; ThermoFisher Scientific). After incubating the plate at 37°C for 6 h, the culture medium was replaced by William's medium (Gibco) supplemented with hepatocytes maintenance supplement pack (CM4000; ThermoFisher Scientific).

### **II-3-7. Detection of secreted human albumin**

The presence of human albumin in the medium was determined by the Human albumin ELISA Kit (Bethyl Laboratories, Texas, USA). The assay procedure was performed according to the supplier's recommendation. The albumin secretion was normalized to culture day and total cell numbers.

### **II-3-8. Measurement of CYP3A4 activity in vitro using LC-ESI/MS/MS system**

To assess the hepatic enzyme activity, 25  $\mu$ M rifampicin (Sigma), which is a CYP3A4 inducer, was treated for 48 h in cells. Next, 20  $\mu$ M midazolam (Sigma), previously reported as the substrate of CYP3A4 [58], was treated for 24 h. Sample preparation involved simple protein precipitation with organic solvent (cold acetonitrile). Briefly, cell samples (50  $\mu$ L) were precipitated with 150  $\mu$ L of cold acetonitrile containing internal standard carbamazepine (CBZ, 10 ng/mL), and agitating with a vortex mixer before centrifugation. Samples were centrifuged at 3400 rpm, 4°C for 20 min and the supernatant samples were analyzed by LC-MS/MS according to the previous publication [59]. Briefly, the LC-

ESI/MS/MS system consisted of an Agilent 1200 series HPLC system (Agilent Technologies, Wilmington, DE, USA) coupled with an API 4000 LC-MS/MS with a Turbo V IonSpray source (Applied Biosystems, Foster City, CA, USA) operated in the positive ion mode. The chromatographic column was conducted on an Atlantis dC18 column (50×2.1 mm i.d., 3 μm, Waters, Milford, MA, USA) with a SecurityGuard C18 guard column (2.0×4.0 mm i.d., Phenomenex, Torrance, CA, USA). The sample injection volume was 5 μL, and the flow rate was set at 0.4 mL/min, and the oven temperature was maintained at 30°C. The mobile phase consisted of HPLC water (A) and acetonitrile (B), each containing 0.1% formic acid. The TurboIonSpray interface was operated in the positive ion mode at 5500 V. The operating conditions were determined as follows: ion source temperature, 600°C; nebulizing gas flow, 50 L/min; auxiliary gas flow, 5.0 L/min; curtain gas flow, 20 L/min; and collision gas (nitrogen) pressure  $3.4 \times 10^{-5}$  Torr. Nitrogen gas was used for the curtain gas (CUR), collision gas (CAD), and nebulizer gas (NEB). The detection was conducted using multiple reaction monitoring (MRM) of the transitions of m/z 342>324 for 1-hydroxymidazolam and m/z 237>194 for carbamazepine (internal standard). Acquisition and analysis of data were performed using Analyst software (ver. 1.5.2, Applied Biosystems, Foster City, CA, USA).

### **II-3-9. Measurement of CYP3A4 activity in vitro using luminescence system**

The enzyme activity was also determined using the P450-Glo CYP3A4 kit (Promega, USA). The experiment was performed according to the supplier's recommendations. The luminescence was measured by SpectraMax® L Luminometer (Molecular Devices, CA, USA). The activity was normalized to the culture day and dsDNA content of each sample.

### **II-3-10. Statistical analysis**

All experiments were performed on at least three ( $n = 3$ ) independent biological samples, and data are presented as means  $\pm$  standard deviations (SD). Statistical analysis was performed using GraphPad Prism 6.0 software (GraphPad Software, CA, USA). Comparisons of three or more data sets were performed by one-way ANOVA followed by Bonferroni's multiple comparison tests. Two-group comparisons were made using two-tailed Student's t-tests.  $P < 0.05$  was considered statistically significant.

## II-4. Results

### II-4-1. *In vitro* hepatic differentiation of four different types of MSC lines

In previous studies of hepatic differentiation, MSCs were differentiated into hepatocyte-like cells (HLCs) using specific growth factors or chemicals, such as hHGF, FGF2, 5-azacytidine (5-aza), Fasudil in step-1, and dexamethasone (DEX), ITS, oncostatin M (OSM) in step-2 [36, 60]. We attempted to differentiate four different MSC lines into HLCs using the previous conventional protocol (Figure. 3A). The hepatic morphological change was observed in all MSC lines at day 14 of differentiation, but human albumin (ALB) was significantly lower in AM-MSCs-derived HLCs (AM-HLCs) compared to other MSC lines (Figure. 3B). Hepatocyte-related gene expression, such as *CPM*, *AFP*, *ALB*, *HNF4A*, and *CYP3A4*, was also lower than UCM-, BM-, and LD-MSCs except for *AFP* at day 14 of differentiation (Figure. 3C and D). Thus, although AM-MSCs have advantages for differentiation, we tried to find the reason why AM-MSCs did not efficiently differentiate into HLCs using transcriptome analysis.

### II-4-2. Transcriptome analysis of AM-MSCs and UCM-MSCs

We tried to differentiate AM-MSCs into HLCs using the conventional protocol, but the efficiency of differentiation was low. The UCM-MSCs were previously reported that the stem cells could be easily differentiated into HLCs because the hepatic development-related gene has already been expressed [61]. Therefore, we analyzed the global transcriptomes in AM-MSCs and UCM-MSCs and compared each other to establish an efficient hepatic differentiation protocol for AM-MSCs. A total of 1,376 genes were differentially expressed between the two stem cell groups (Figure. 4A). Although AM-MSCs and UCM-MSCs were the same embryonic origin, transcriptome profiles were different (Figure. 4B). We also performed GO-term enrichment analysis to classify the genes with similar genetic functions in the biological process. The result showed that the genes differentially expressed between the two types of stem cells fell into several different biological categories, such as biological regulation, metabolic process, response to stimulus, signaling, and developmental process (Figure. 4C).

Finally, we compared hepatic development-associated genes in the two other stem cells. The result showed that *GATA6*, *KIT*, *AFP*, *c-MET*, *FGF2*, *EGF*, and *c-JUN* were down-regulated and *GSK3A* was up-regulated in AM-MSCs ( $P < 0.05$ , Figure. 4D). In summary, AM-MSCs were originated from embryos like UCM-MSCs, but the gene expression profiles were different. In particular, the genes, such as *GATA6*, *EGF*, *AFP*, *FGF2*, and *GSK3*, involved in hepatic development were not properly expressed. Thus, we hypothesized that it is the reason why AM-MSCs are difficult to differentiate using the conventional protocol.

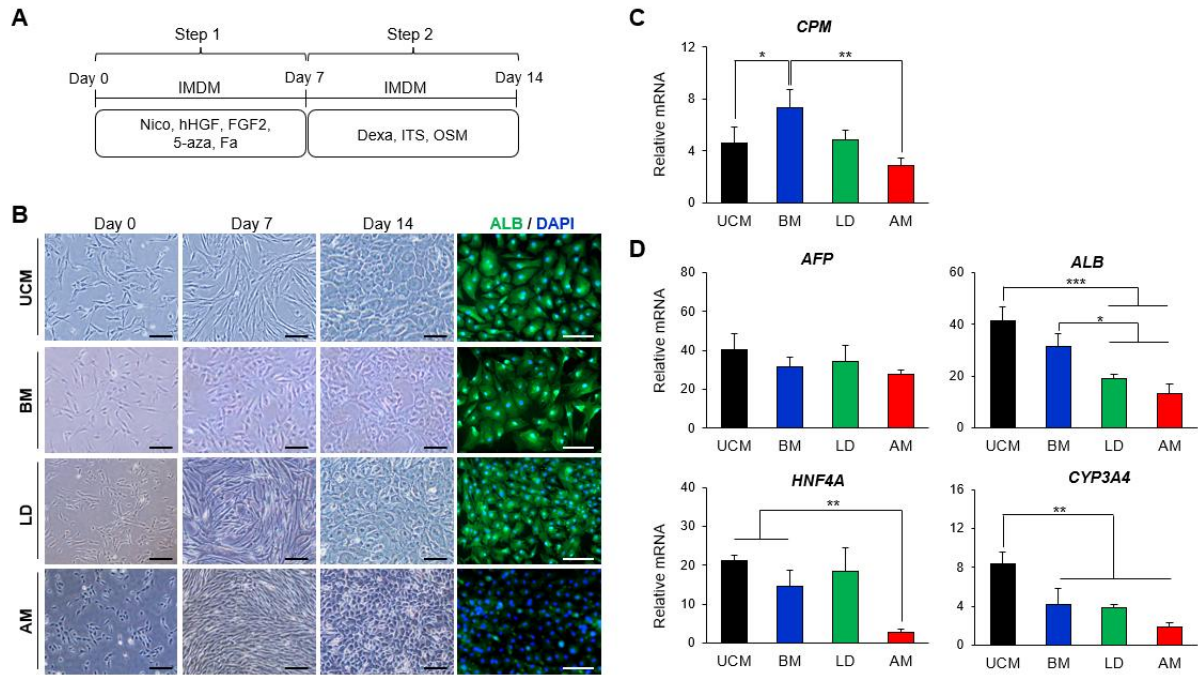


**Figure 7. Hepatic generation of human mesenchymal stem cells using the conventional method.**

(A) The experimental scheme of conventional *in vitro* hepatic differentiation protocols. (B) Morphology of cells during hepatic differentiation on days 0, 7, and 14 (Scale bar = 150  $\mu$ m), and immunostaining of ALB expression on day 14 (Scale bar = 200  $\mu$ m). Green, ALB; Blue, DAPI. (C) RT-qPCR analysis of selected hepatic progenitor markers, *CPM*. (D) Relative mRNA Expression of early hepatic (*AFP*) and hepatic maturation (*ALB*, *HNF4A*, and *CYP3A4*) markers on day 14 of the differentiated cells. *GAPDH* was used as an internal control for RT-qPCR. P-values < 0.05 were considered significant. \*, P < 0.05; \*\*, P < 0.01, \*\*\*, P < 0.001.

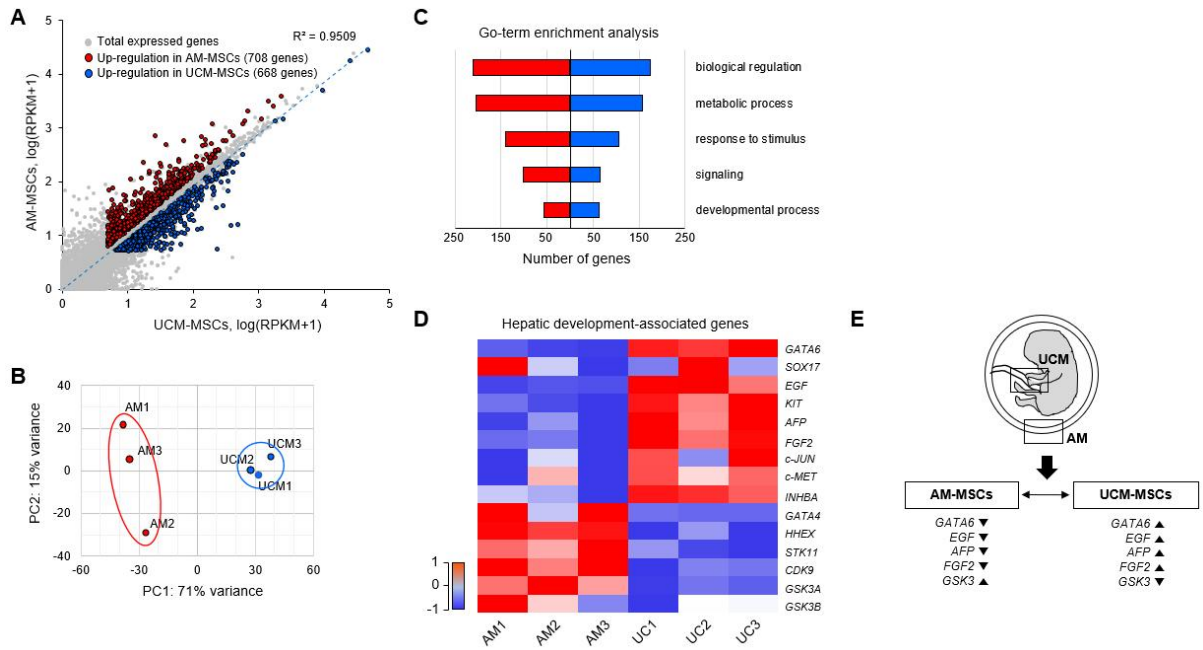


**Figure 8. Transcriptome analysis in UCM-MSCs and AM-MSCs.**

(A) The correlation plot of RPKM values between UCM-MSCs ( $n = 3$ ) and AM-MSCs ( $n = 3$ ). In the plot, the RPKM values were exchanged by  $\log(\text{RPKM}+1)$ . A total of 708 genes is more highly expressed in AM-MSCs and 668 genes relatively low expressed. (B) PCA plots of transcriptome analysis in UCM-MSCs ( $n = 3$ ) and AM-MSCs ( $n = 3$ ). (C) GO-term enrichment analysis, based on biological process (BP), of genes, differentially expressed between AM-MSCs and UCM-MSCs. Significantly highly expressed genes in AM-MSCs are highlighted in red, while blue represents DEGs in UCM-MSCs. (D) Heat map of hepatic development-associated gene expression in AM-MSCs ( $n = 3$ ) and UCM-MSCs ( $n = 3$ ). (E) Summary of transcriptome analysis, which related to hepatic development, in UCM-MSCs and AM-MSCs.

### II-4-3. Analysis for increasing the efficient hepatic differentiation

After transcriptome analysis, we hypothesized that *GSK3* and *GATA6* were key genes for efficient hepatic differentiation of AM-MSCs. Because the high levels of *GSK3* and low levels of *GATA6* could repress the induction of definitive and hepatic endoderm [62]. Induction of endoderm has been known to be significantly important for hepatic differentiation in previous studies [60]. Therefore, to establish an efficient hepatic differentiation protocol, we tried to induce and inhibit the genes using chemicals.

First, we conducted a quantitative PCR to confirm the expression levels of *GATA6* in AM-MSCs and UCM-MSCs. *GATA6* was much lower in all three AM-MSC lines than in UCM-MSCs ( $P < 0.001$ , Figure. 5A). Then, we searched for a chemical that increased *GATA6* and inhibited *GSK3*. CHIR99021 (CHIR), also known as *GSK3* inhibitor, could induce *GATA6* expression for hepatic differentiation from human embryonic stem cells [63, 64]. Also, down-regulated *GSK3* could induce upregulation of *GATA6* [65]. Therefore, we tested the CHIR effect on AM-MSCs. CHIR was treated for 2 days and measured the expression of *GATA6*, and *SOX17*, which is known as the definitive endodermal marker. As we expected, these two genes showed significantly increased expression in the w/CHIR group than control ( $P < 0.01$ , Figure. 5B). Based on results, we hypothesized that inhibition of *GSK3* could increase the expression of *GATA6* and induction of endoderm, and sequentially enhance the efficiency of hepatic differentiation (Figure. 5C). Finally, we conducted the differentiation with CHIR and various supplements (Figure. 5D).

### II-4-4. Efficient *in vitro* hepatic differentiation protocol

To establish an efficient *in vitro* hepatic differentiation protocol, we investigated the effect of adding various factors along with CHIR to increase the expression of *GATA6* and *SOX17*. Epidermal growth factor (EGF) and dexamethasone (Dexa) play an important role in hepatic biology and maturation [66]. Insulin-transferrin-selenite (ITS) and fasudil (Fa) also enhance the stability of stem cell cultures and their differentiation [67]. Based on these factors, we modified the conventional to the advanced protocol by adding CHIR, Dexa, ITS, and EGF on step-1, and hHGF, Fa on step-2 (Figure. 6A). In response, the expression of *GATA6* and *SOX17* was significantly increased on day 2 when the advanced protocol was used ( $P < 0.001$ , Figure. 6B). Therefore, we efficiently and successfully induced definitive endoderm for hepatic differentiation. Finally, we observed cell morphology and stained it for ALB expression. The oval or polygonal-like structure of the cells was similar, but ALB was more highly expressed on day 14 (Figure. 6C).

We also analyzed the hepatic gene expression and confirmed that the differentiation efficiency



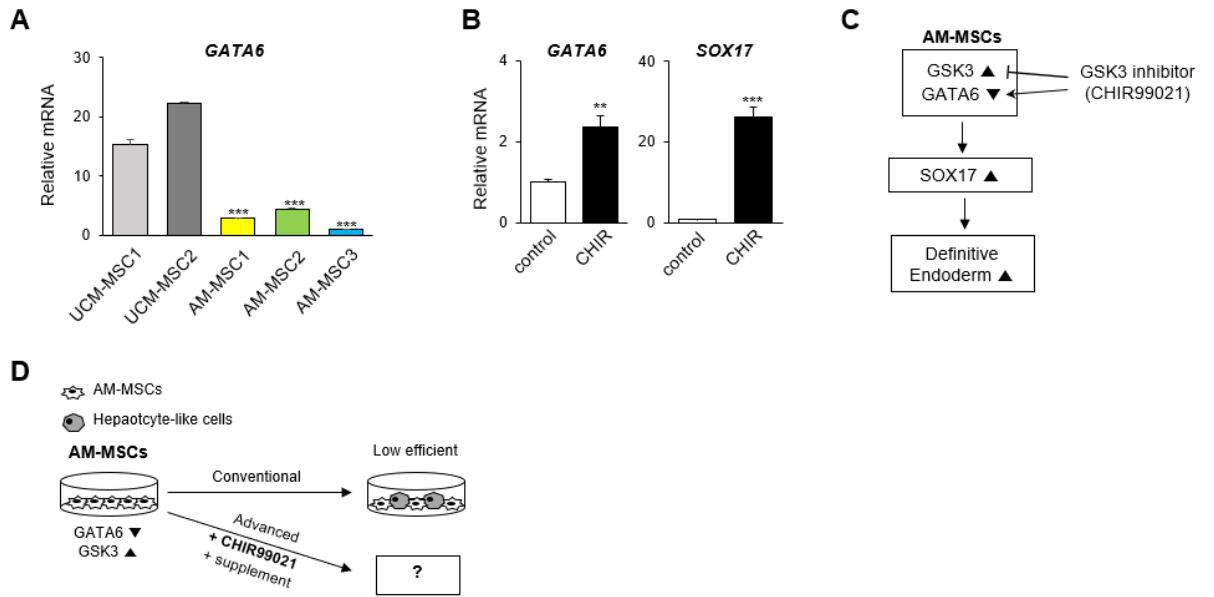


**Figure 9. Enhancing the endoderm differentiation potent based on the transcriptome analysis.**

(A) RT-qPCR analysis of GATA6 in AM-MSCs (n = 3) and UCM-MSCs (n = 2). (B) Analyzing the regulation of GATA6 and SOX17 in AM-MSCs with or without CHIR99021 by RT-qPCR. *GAPDH* was used as an internal control for RT-qPCR. P-values < 0.05 were considered significant. \*, P < 0.05; \*\*, P < 0.01, \*\*\*, P < 0.001. (C) The schematic mechanism of the effect of GSK3 inhibitor (CHIR99021) on AM-MSCs. (D) Summary and scheme of further experiments.

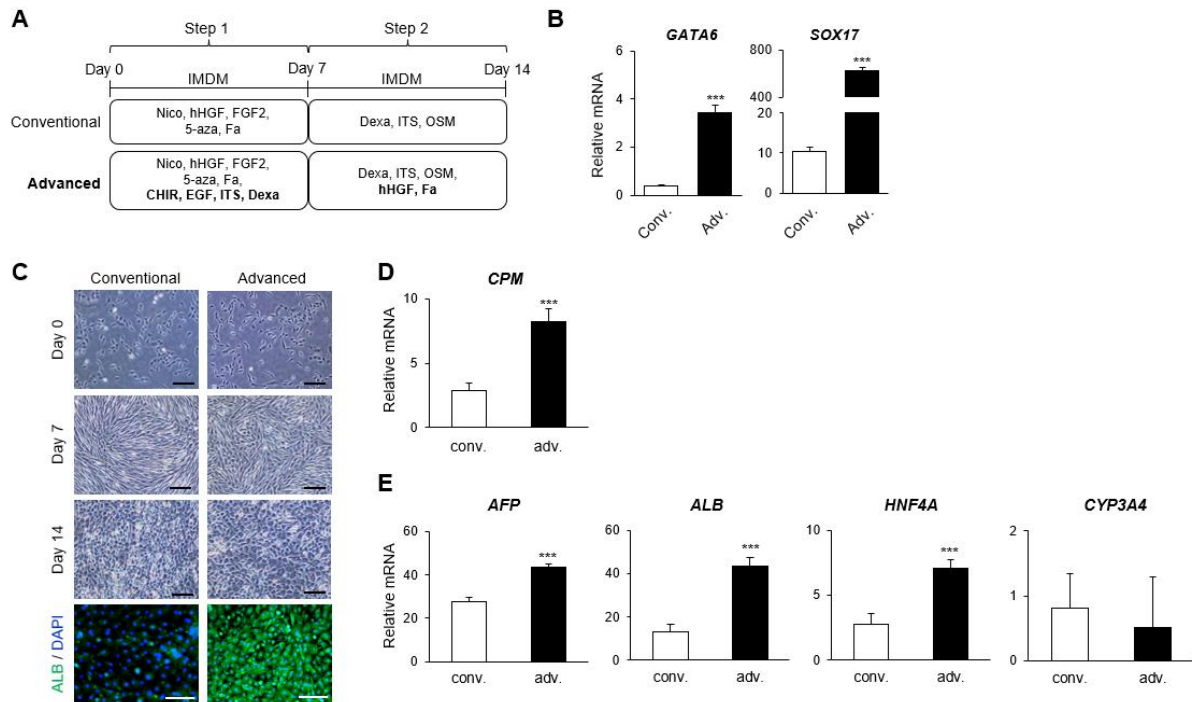


**Figure 10. Advanced protocol for enhancing the hepatic differentiation of AM-MSCs.**

(A) Comparison of components in each hepatic differentiation protocol, conventional versus advanced. The different components in the advanced protocol were highlighted in bold. (B) Analyzing the effect of the different protocols on the regulation of GATA6 and SOX17 in AM-MSCs by RT-qPCR. (C) Morphology of cells during hepatic differentiation on days 0, 7, and 14 and immunostaining of ALB expression on day 14 (Scale bar = 200  $\mu$ m). Green, ALB; Blue, DAPI. (D) RT-qPCR analysis of hepatic progenitor marker (*CPM*), (E) early hepatic (*AFP*), hepatocyte-related markers (*ALB*, and *HNF4A*), and hepatic metabolism marker (*CYP3A4*). *GAPDH* was used as an internal control for RT-qPCR. P-values < 0.05 were considered significant. \*, P < 0.05; \*\*, P < 0.01, \*\*\*, P < 0.001. Abbreviation: Conv., conventional protocol; Adv., advanced protocol.

was increased by using the advanced protocol. The expression of *CPM*, *AFP*, *ALB*, and *HNF4A* was more highly expressed on day 14 in the advanced protocol ( $P < 0.001$ ), while the expression of *CYP3A4* was comparable (Figure. 6 D and E). Therefore, we established the efficient hepatic differentiation protocol.

#### **II-4-5. The use of PVA for xeno-free hepatic differentiation**

FBS is still widely used for inducing hepatic differentiation [68]. However, it causes an acute immune response after transplantation because of xeno-contamination. Therefore, we substituted 0.1% PVA for 1% FBS in the advanced protocol (Figure. 7A). The phenotype of differentiated cells was similar, and *ALB* was expressed when both PVA and FBS were used (Figure. 7B). We also analyzed the expression of hepatocyte-related genes on day 14 using previous reports [69]. and compared with primary hepatocytes (PHH) and UCM-HLCs, which were differentiated by conventional protocol, for assessment of differentiation efficiency. *CPM*, which is related to hepatic progenitor markers, was expressed more highly in the PVA group on day 14 ( $P < 0.001$ , Figure. 7C). We also analyzed the genes, which are associated with liver-specific plasma, a nuclear protein, and metabolisms such as *AFP*, *ALB*, *HNF4A*, and *CYP3A4*. The levels of expression of *AFP*, *ALB*, *HNF4A*, and *CYP3A4* also were higher in the PVA group on day 14 ( $P < 0.05$ , Figure. 7D). Moreover, *HNF1A*, *CYP1A2*, *UGT1A6*, *MRP2*, and *ASGR1* were expressed higher in the PVA group on day 14 ( $P < 0.05$ , Figure. 7E). When compared to UCM-HLCs, the differentiation efficiency was similar or significantly increased. However, compared with primary hepatocytes, PHH was a significantly lower expression of *CPM*, and *AFP* ( $P < 0.05$ ), while *HNF1A* and *UGT1A6* were comparable. The other genes were higher than on day 14 of the PVA group ( $P < 0.05$ ).

Moreover, to confirm that the PVA-advanced protocol increases the differentiation efficiency on other MSC lines, we applied the protocol to UCM-MSCs. The efficiency of hepatic differentiation was significantly increased than the conventional one (Figure. 8).

#### **II-4-6. The hepatic functions of AM-HLCs**

The main functions of hepatocytes are protein synthesis and detoxification. It is important to confirm the function of differentiated cells for use in stem cell therapy. Thus, we performed to measure albumin secretion and *CYP3A4* activity in media cultured AM-HLCs. First, we confirmed the protein expression of *ALB* and *CYP3A4* in AM-HLCs. At 18 days after differentiation and maturation, *ALB* and *CYP3A4* were successfully expressed in AM-HLCs (Figure. 9A). Next, we confirmed that the secretion of human

albumin was significantly increased on day 18 of AM-HLCs than day 0 of undifferentiated cells, but less secreted than PHH control ( $P < 0.05$ , Figure. 9B).

To confirm the detoxification function of AM-HLCs, we measured the CYP3A4 activity using two independent methods. First, we used a luminescence system. In the system, CYP3A4 activity was increased in the AM-HLCs compared with undifferentiated cells, but less activated than PHH control ( $P < 0.01$ , Figure 9C). We also used the LC-ESI/MS/MS system for measuring the CYP3A4 activity [59]. In this system, we treated the substrate of CYP3A4, midazolam, to AM-MSCs (undifferentiated cells) and AM-HLCs for 24 hours and measured the metabolite of midazolam, 1-hydroxymidazolam, using the system. The metabolite was only detected in the AM-HLCs, and it significantly increased on day 18 differentiated HLCs, but less activated than PHH control ( $P < 0.05$ , Figure. 9 D and E) These results suggest that the differentiated hepatic cells with PVA-advanced protocol are useful for transplantation into diseased livers because the cells produced albumin and CYP3A4 enzyme, which could catalyze toxic drugs in the liver [70].

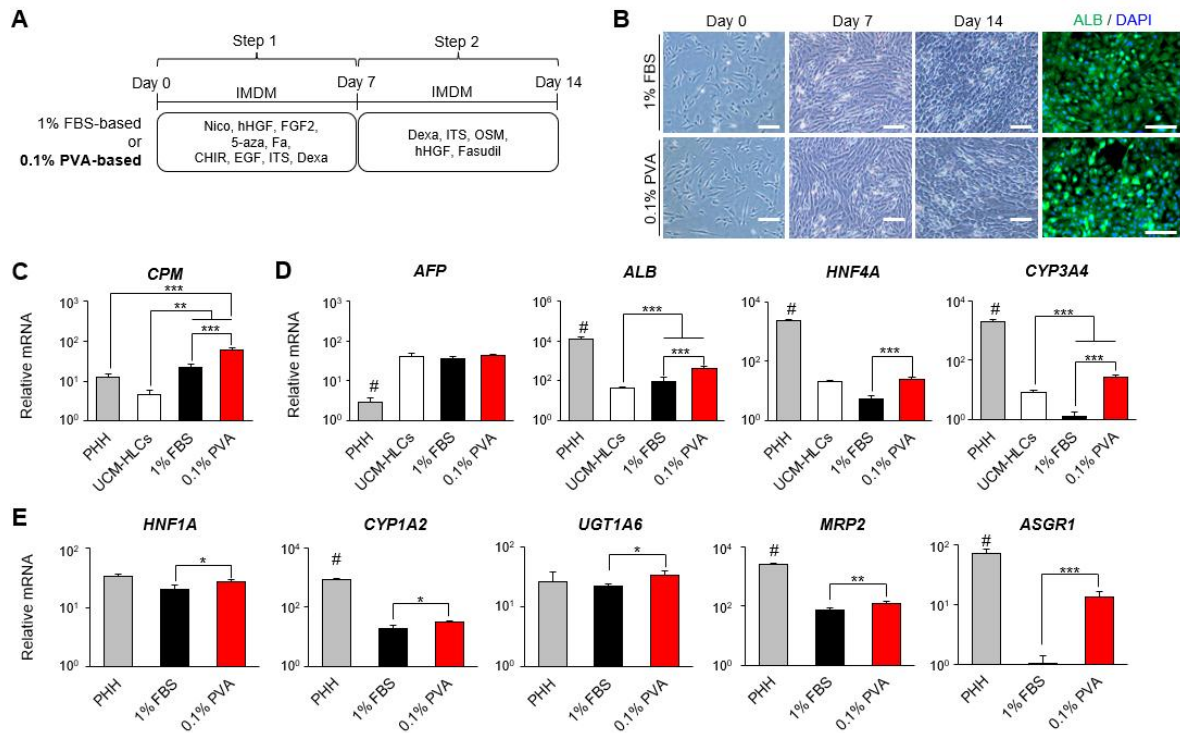


**Figure 11. Serum-free hepatic differentiation using PVA.**

(A) Scheme for hepatic differentiation using 0.1% PVA or 1% FBS in the advanced protocol. (B) Morphological change of cells during hepatic differentiation on days 0, 7, and 14 (Scale bar = 150  $\mu$ m), and immunostaining of ALB expression on day 14 (Scale bar = 200  $\mu$ m). Green, ALB; Blue, DAPI. (C-E) The mRNA expression levels of hepatic progenitor marker (*CPM*), liver-specific plasma and nuclear protein (*AFP*, *ALB*, *HNF1A*, and *HNF4A*), and liver-specific metabolism (*CYP1A2*, *CYP3A4*, *UGT1A6*, *MRP2*, and *ASGR1*) in PHH, UCM-HLCs, PVA- and FBS-used AM-HLCs group. P-values < 0.05 were considered significant. '#' means that PHH was compared with the other cells. #, P<0.05; \*, P < 0.05; \*\*, P < 0.01, \*\*\*, P < 0.001.

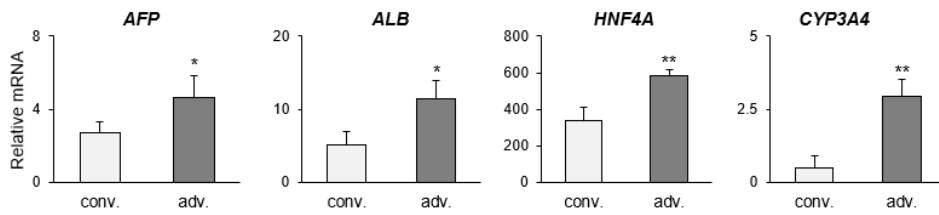


**Figure 12. The effect of advanced protocol on UCM-MSCs**

Comparison of the relative mRNA expression in hepatic differentiated UCM-MSCs using two different protocols. *CPM*, hepatic progenitor marker; *AFP*, early hepatic marker; *ALB* and *HNF4A*, hepatocyte-related markers; *CYP3A4*, hepatic metabolism marker. *GAPDH* was used as an internal control for RT-qPCR. P-values < 0.05 were considered significant. \*, P < 0.05; \*\*, P < 0.01, \*\*\*, P < 0.001. Abbreviation: Conv., conventional protocol; Adv., advanced protocol.

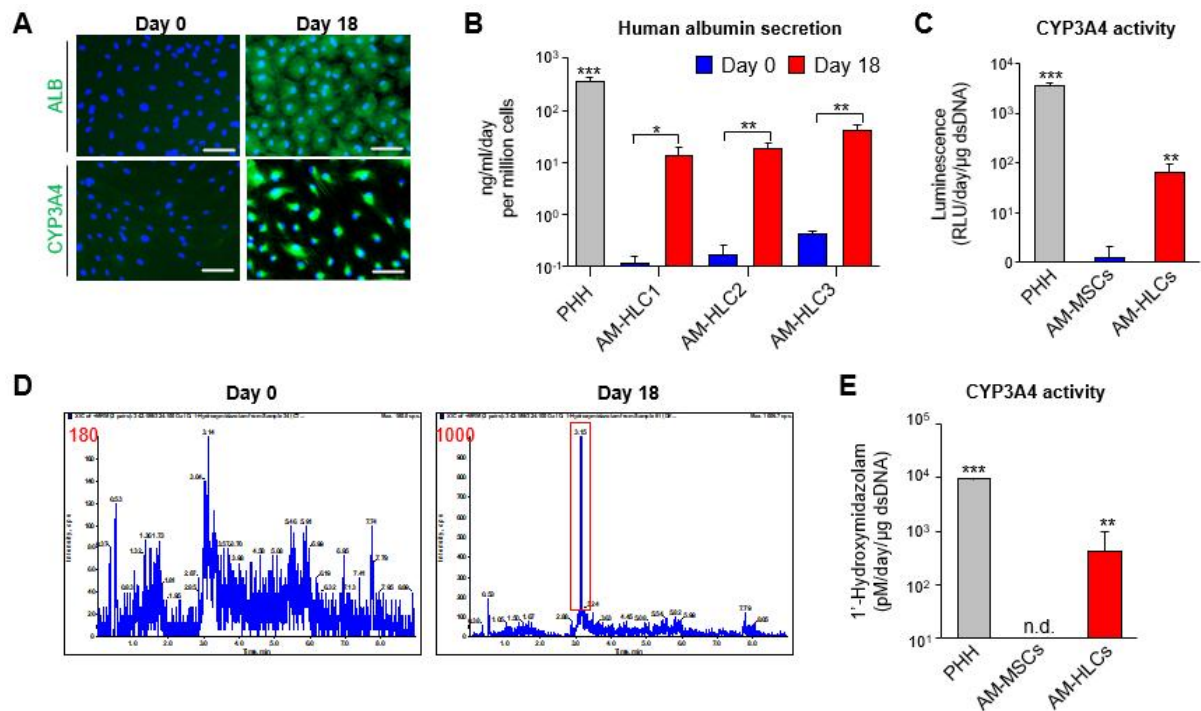


**Figure 13. The hepatic function of AM-derived hepatocyte-like cells induced by PVA-used protocol.**

(A) Detection of ALB and CYP3A4 in undifferentiated cells (day 0) and differentiated cells (hepatocyte-like cells; day 18). Green, ALB, and CYP3A4. Blue, Nuclear. Scale bar = 100  $\mu$ m. (B) Measurement of human secreted albumin in three different donor-derived AM-HLCs and PHH. (C) CYP3A4 enzyme activity measurement using luminescence systems in PHH, AM-MSCs, and AM-HLCs. (D) Chromatogram of LS-ESI/MS/MS profiles in the culture medium of each group, undifferentiated cells (day 0) and differentiated cells (day 18), after treating midazolam. Red box: the peak of 1-hydroxymidazolam. (E) Measurement of CYP3A4 enzyme activity using LC-ESI/MS/MS systems in PHH, AM-MSCs, and AM-HLCs. P-values < 0.05 were considered significant. \*, P < 0.05; \*\*, P < 0.01, \*\*\*, P < 0.001.

#### **II-4-7. Summary of *in vitro* hepatic differentiation**

In *in vitro* studies, we have successfully and efficiently differentiated the AM-MSCs into AM-HLCs using a newly developed method (Figure. 11). AM-MSCs had various advantages, such as cell size, pluripotency, immunomodulation, and mitochondria function, compared to four other types of MSC lines. However, it was difficult to differentiate into HLCs because of their transcriptome characters. AM-MSCs had low expression levels of hepatic development-related genes (*GATA6*, *EGF*, *AFP*, and *FGF2*) and high expression levels of *GSK3*. These profiles are a critical obstacle for liver differentiation. Therefore, we added the small molecule, CHIR99021, and various supplements, such as dexamethasone, ITS, EGF, and Fa, to conventional protocol. CHIR induced the expression of *GATA6* and *SOX17*, which were necessary genes for stem cells to differentiate into hepatocytes. Probably, *GSK3* inhibited by CHIR activated *GATA6* signaling, which upregulated the Wnt/ $\beta$ -catenin pathway, leading to the enhancement of the *SOX17* gene [65, 71, 72]. Moreover, we made the xeno-free advanced protocol by alternating FBS to PVA. In the advanced protocol, AM-MSCs were successfully differentiated into HLCs, and the genes, which were associated with the hepatic progenitor, hepatic characters, and metabolism, were significantly increased. Finally, we confirmed that the hepatic functions, such as albumin secretion and CYP3A4 activity, were normally induced in AM-HLCs



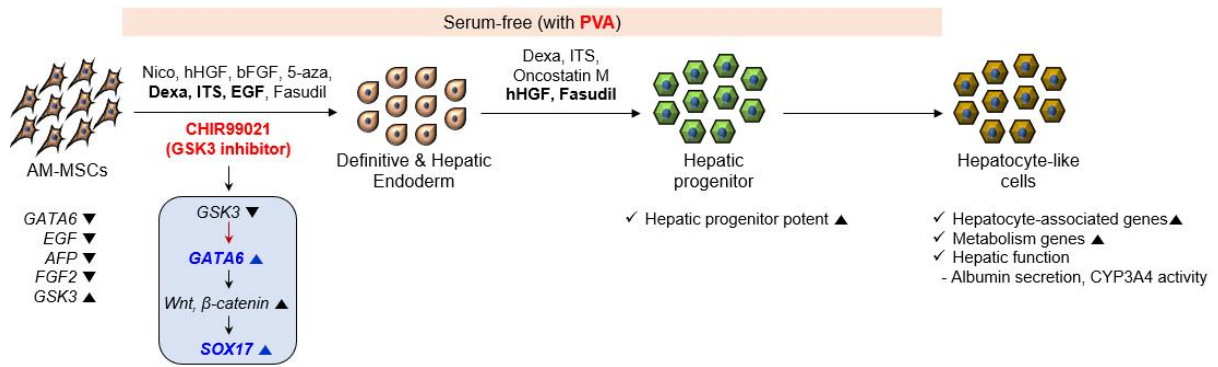


**Figure 14. Schematic summary of *in vitro* study**

**Chapter III.**  
**The study of**  
***in vivo* hepatic transplantation and**  
**regeneration**

### **III-1. Abstract**

It is important to pre-clinically test the transplantation effect on a mouse model for clinical trials of cell therapy. Therefore, in this part, we tested the therapeutic effect of AM-derived hepatic progenitors (HPCs), which were differentiated by PVA-advanced protocol, on the newly established acute hepatic failure mouse model. The previous thioacetamide (TAA)-the induced model had disadvantages. The mouse easily died when high dose used, while the induction of model was not completely induced when low dose used. Therefore, in order to improve the mouse model, we injected the cyclophosphamide (CTX) into the mouse model 24 hours after injecting the TAA. As a result, indicators of liver disease, ALT and ALT (GOT), were successfully increased compared with TAA only model, and the levels of hemoglobin (HGB) and red blood cells (RBC) have stably existed. Finally, to test the transplantable potential of HPCs, we optimized the transplantation date based on the expression of the HPC-related gene and mitochondrial function. At 12 days after differentiation, the differentiated cells were most suitable for transplantation. Finally, we conducted the transplantation study. When the AM-HPCs were transplanted into the liver failure mouse model, they settled in and cured the damaged livers. In conclusion, AM-HPCs could be used as transplantable therapeutic materials and promising cells for treating liver disease.

**Key words:** Liver failure mouse model, Hepatic progenitor, Transplantation, Regeneration

## III-2. Introduction

Testing the safety of cell therapy, based on stem cells or differentiated cells, is an important consideration in the clinical setting. Various animal studies have been previously performed, and these preclinical results led to the initiation of clinical trials. Therefore, preclinical studies are mandatory to assess the risk of a new therapy and predict safety, feasibility, and efficacy. Moreover, they can be tested unresolved issues of clinical tests, such as choice of cell type, appropriated injection cell number, method of delivery, time of delivery, and follow-up studies after cell transplantation [73].

Considering the high predominance of liver disease worldwide, animal models are crucial for improving our understanding of the human liver disease, such as chronic or acute hepatic failure [74]. These studies are enabled to identify and test therapeutic methods, such as cell therapy and drug. In this study, we used an acute liver disease model which was induced by thioacetamide (TAA). TAA is the second most widely used model of hepatotoxin-induced advanced chronic liver disease (ACLD) or acute liver disease. It generates highly reactive metabolites, which bind to proteins and lipids, in the liver, and causes oxidative stress and necrosis [75]. There are various published protocols of TAA-induced cirrhosis with differences in dose and frequency of administration. However, this method only reaches fibrosis or an early stage of cirrhosis in low doses, and mice can easily die when high doses are used [76].

In this part, we established the stable mouse model modified the by addition of cyclophosphamide (CTX) which is also toxic to the bone marrow and liver tissue [77]. Then, to transplant the AM-derived hepatic progenitors into the mouse model, we measured the expression of the carboxypeptidase M (*CPM*) and the oxygen consumption rate of mitochondria for optimizing the transplantation date.

### **III-3. Materials and Methods**

#### **III-3-1. Transplantation experiments**

To establish an acute liver failure model, eight-week-old male C57BL/6 or NOD. Cg-Prkdc<sup>scid</sup> Il2rg<sup>tm1Wjl</sup>/SzJ (NSG) mice were injected intraperitoneally with 0.08 mg/g thioacetamide (TAA; Sigma Aldrich) or an additional 0.025 mg/g cyclophosphamide monohydrate (CTX; Sigma Aldrich) after 24 h. Next, the cells with various stages were transplanted via the intrasplenic route ( $5 \times 10^5$  cells per mouse) of NSG. All mice were purchased from JOONG AH BIO (Suwon, Korea). The mouse study was approved by the Asan Institutional Animal Care and Use Committee (IACUC, 2018-12-167, 2019-12-062, and 2020-02-208).

#### **III-3-2. Blood analysis**

Complete blood counts (CBC) and analyses of peripheral blood from mice were performed using an ABC-VET (Scilvet, Germany) and FUJI DRI-CHEM clinical chemistry analyzer (FUJI, Japan), respectively, at AniCom Medical Center (Seoul, Korea).

#### **III-3-3. Histological staining and analysis**

The retrieved liver tissues were fixed in 3.7% formaldehyde and embedded in paraffin. The paraffin blocks were sectioned at 4  $\mu$ m-thick. To assess acute liver failure in chemically treated mice, the paraffin sections were stained with hematoxylin and eosin (H&E) and scored by Suzuki's method [78]. Three weeks after transplantation, liver repopulation and regeneration were assessed by H&E staining, and immunohistochemistry (IHC). Human albumin was stained with DAB substrate using the previously described IHC methods [36]. Histological images were obtained by light microscopy using an Olympus DP27 (Olympus, Melville, NY, USA).

#### **III-3-4. *In vitro* differentiation of hepatic differentiation**

Stem cells were differentiated from the established PVA-advanced protocol. Briefly, in the advanced protocol, the cells were seeded on 0.1% gelatin-coated dishes at 7000 cells/cm<sup>2</sup> in a cell culture medium. After two days, they were cultured for seven days with Step-1 medium consisting of Iscove's Modified Dulbecco's Medium (IMDM; Gibco) supplemented with 0.1% PVA (Sigma Aldrich), 10 mM nicotinamide (Sigma Aldrich), 20 ng/ml hHGF (Peprotech), 10 ng/ml FGF2, 2  $\mu$ M 5-azacytidine (Sigma Aldrich), 0.1  $\mu$ M dexamethasone (Sigma Aldrich), 1% ITS (Gibco), 3  $\mu$ M CHIR99021, 20 ng/ml EGF (Peprotech), and 10  $\mu$ M Fasudil (AadoQ Bioscience, Irvine, CA, USA). For hepatic progenitor, the Step-

1 medium was replaced with Step-2 medium consisting of IMDM supplemented with 1  $\mu$ M dexamethasone, 1% ITS, 20 ng/ml Oncostatin M (OSM, Peprotech), 20 ng/ml hHGF, and 10  $\mu$ M Fasudil for 10, 12, and 14 days.

### III-3-5. Immunofluorescence staining

Transplanted liver tissues were fixed in 3.7% formaldehyde overnight at 4°C, incubated overnight at 4°C in 30% sucrose, overlaid with OCT compound, and frozen in liquid nitrogen. The frozen blocks were sectioned with a cryotome of 10  $\mu$ m thickness. The sections were permeabilized with 0.2% Triton X-100/PBS for 30 min at RT, blocked with 10% FBS buffer at RT in a humidity chamber, and stained overnight with anti-human albumin diluted 1:100 at 4°C in the humidity chamber. The secondary antibody was goat anti-mouse IgG H&L Alexa Fluor® 647; Abcam, 1:100). Nuclei were counterstained with 4', 6-diamidino-2-phenylindole (DAPI) for 10 min, and fluorescence signals were detected using an AxioObserver Z1 microscope.

### III-3-6. Human mitochondrial DNA detection

Total DNA was isolated with a PicoPure™ DNA extraction kit (Thermofisher Scientific). The PCR reaction was conducted using 2x PCR BIO HS Taq Mix Red (PCRbiosystems) with 300 ng of DNA in a total volume of 20  $\mu$ l. The reaction was performed as described in the kit with annealing at 56 °C for 20 seconds. Sanger sequencing of the PCR products of injected cells and transplanted cells was carried out by MacroGen (Seoul, Korea).

Gene name	Primer sequence (5' to 3')	*F, Forward; R, Reverse
<i>Human mitochondrial DNA</i>	F: CAACACTAAAGGACGAACCTGA R: TCGTAAGGGGTGGATTTTC	

### III-3-7. Evaluation of transplant efficiency

To determine the percentage of engrafted human cells in the mouse liver, each standard curve of human or mouse mtDNA was prepared by quantitative real-time PCR (qPCR). For preparing the standard curve, both DNA concentrations were measured by NanoDrop™ 2000/2000c Spectrophotometer (Thermofisher Scientific), and samples with OD 260/280 between 1.8-2.0 were used for further analysis. The DNA concentration was diluted by DNase-free water to the following concentration, 1000, 100, 10, and 1 ng/ $\mu$ l. The qPCR was performed using 1  $\mu$ l of the diluted DNA (1000, 100, 10, and 1 ng) and Power SYBR® Green PCR Master Mix on a QuantStudio™ real-time PCR System. After finishing the qPCR, the standard curve of human or mouse mtDNA was made using the diluted DNA concentration

(X-axis) and CT value (Y-axis) (Figure. 15B). Finally, human and mouse mtDNA concentrations were acquired through the standard curve in transplanted samples, and the percentage of transplantation efficiency was calculated following formula:  $[\text{human mtDNA} / (\text{mouse mtDNA} + \text{human mtDNA})] \times 100$  (%). The primer sequences used in the experiment were described below the table.

Gene name	Primer sequence (5' to 3')	*F, Forward; R, Reverse
<i>Human mitochondrial DNA</i>	F: CAACACTAAAGGACGAACCTGA R: TCGTAAGGGGTGGATTTTC	
<i>Mouse mitochondrial DNA</i>	F: CCCAAGACAACCAACCAAAA R: ACTAGCTTATATGCTTGGGG	

### III-3-8. Statistical analysis

All experiments were performed on at least three (n = 3) independent biological samples, and data are presented as means  $\pm$  standard deviations (SD). Statistical analysis was performed using GraphPad Prism 6.0 software (GraphPad Software, CA, USA). Comparisons of three or more data sets were performed by one-way ANOVA followed by Bonferroni's multiple comparison tests. Two-group comparisons were made using two-tailed Student's t-tests. P <0.05 was considered statistically significant.

## III-4. Results

### III-4-1. Acute hepatic failure mouse model

The AM-derived differentiated cells were transplanted into the mouse liver failure model to see whether the cells could engraft into functional hepatocytes *in vivo*. To start with, the protocol to induce liver damage in mice was modified with the inclusion of cyclophosphamide monohydrate (CTX) along with thioacetamide (TAA). TAA is widely used in mice to induce liver failure. However, it requires close monitoring and supportive care of the mice due to lethality before research start [79]. In previous studies, the mice which received the highest doses (0.2–0.4 mg/g) of TAA died before the start of the study, and the mice were not well-induced at lower doses. Therefore, we needed a more stable mouse model for transplantation studies.

CTX is also toxic to the bone marrow and liver tissue [77]. Based on previous studies, we devised an improved acute liver failure model using 0.025 mg/g CTX and 0.08 mg/g TAA (Figure. 12A). To demonstrate the improvement, whole blood was collected from the mouse model and analyzed complete blood counts (CBC) and hepatic blood enzyme analyzes were 24 hours after induction of disease. In the result of CBC, the percentage of lymphocytes was significantly decreased in both groups ( $P < 0.01$ ), TAA only and CTX+TAA, while hemoglobin (HGB) and red blood cells (RBC) in the CTX+TAA group were compatible with the vehicle group (Figure. 12B). Decreasing the levels of RBC and HGB in the mouse can lead to death. The markers for liver damage, alanine aminotransferase (ALT), and aspartate aminotransferase (AST-GOT), were significantly increased in CTX+TAA treated groups compared with the vehicle group ( $P < 0.001$ ). Furthermore, both ALT and AST were significantly more highly expressed in the CTX + TAA group compared with the TAA-only model ( $P < 0.001$ , Figure. 12C), while the liver damage has occurred similar around the hepatic vein (Figure. 12D). The modified model had a similar effect on acute liver failure as the TAA model, but the Suzuki score tended to be higher (Figure. 12E), and the latter appears to be the historical criterion for assessing liver injury [78]. In conclusion, the newly modified mouse model can be safely used for the study without many deaths of mice. Thus, we decided to transplant the differentiated cells into the mouse model.

### III-4-2. Optimization of transplantation date

Bipotent hepatic progenitor cells provide more efficient rehabilitation than mature hepatocytes after transplantation [80]. To decide a suitable transplantation time for the AM-MS-C-derived hepatic progenitor cells (AM-HPCs) *in vivo*, we conducted two experiments to examine the functional properties of the HPCs. First, we investigated the highest expression date of *CPM*, which are critical



markers for bi-potential hepatic progenitor cells that can be differentiated into hepatocytes or cholangiocytes [81]. The *CPM* was most highly expressed on day 12 ( $P < 0.001$ , Figure. 13A). Second, we observed mitochondrial oxygen consumption rates (OCR) on days 7, 10, 12, and 14 following differentiation using PVA. Overall OCR levels were highest on day 12; more specifically, maximal respiration, spare respiratory capacity, and ATP production were significantly elevated on day 12 ( $P < 0.01$ , Figure. 13B). Spare respiratory capacity is the extra-mitochondrial capacity, which is available under conditions of increased work or stress. Also, it is considered important for long-term cell survival and function [82]. As a result, the cells on day 12 of differentiation were most close to the hepatic progenitor and were in a suitable state for *in vivo* transplantation. In conclusion, we decided to transplant the cells, which were differentiated into HPCs for 12 days, into the acute hepatic failure mouse model.

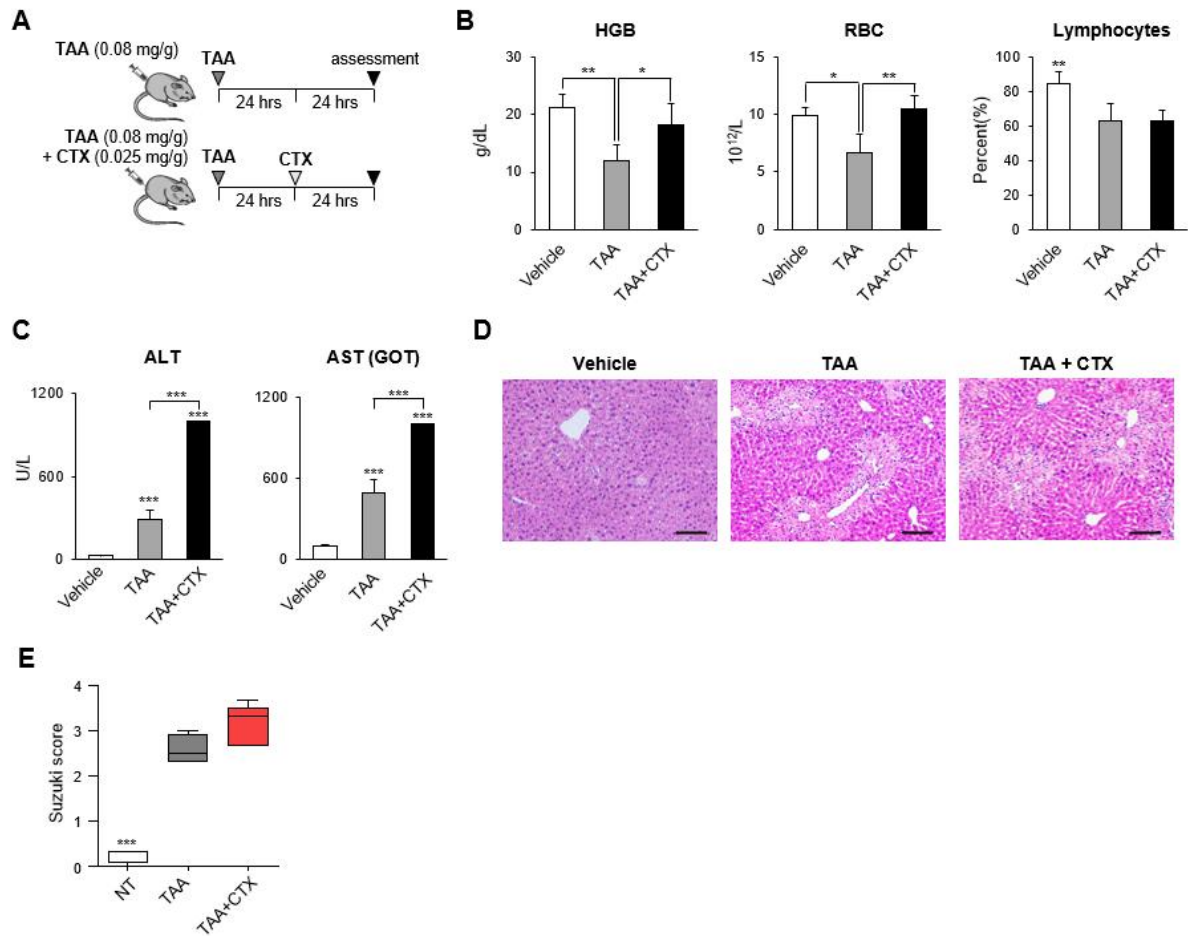


**Figure 15. Modification of acute liver failure mouse model.**

(A) Schematic summary of the modified acute liver failure mouse model. To establish the new model, we used a C57BL/6 mouse in this experiment. (B) Complete blood counts of hemoglobin (HGB), red blood cells (RBC) and lymphocytes in vehicle (n = 4), TAA (n = 4), and TAA + CTX group (n = 5). (C) Blood hepatocyte-related enzyme analysis in vehicle (n = 4), TAA (n = 4), and TAA + CTX group (n = 5). (D) Representative hematoxylin and eosin (HE) staining in vehicle, TAA, and TAA + CTX group. Scale bar = 200  $\mu$ m. (E) Hepatic failure score (suzuki score) in vehicle (n = 4), TAA (n = 4), and TAA + CTX group (n = 5). P-values < 0.05 were considered significant. \*, P < 0.05; \*\*, P < 0.01, \*\*\*, P < 0.001.

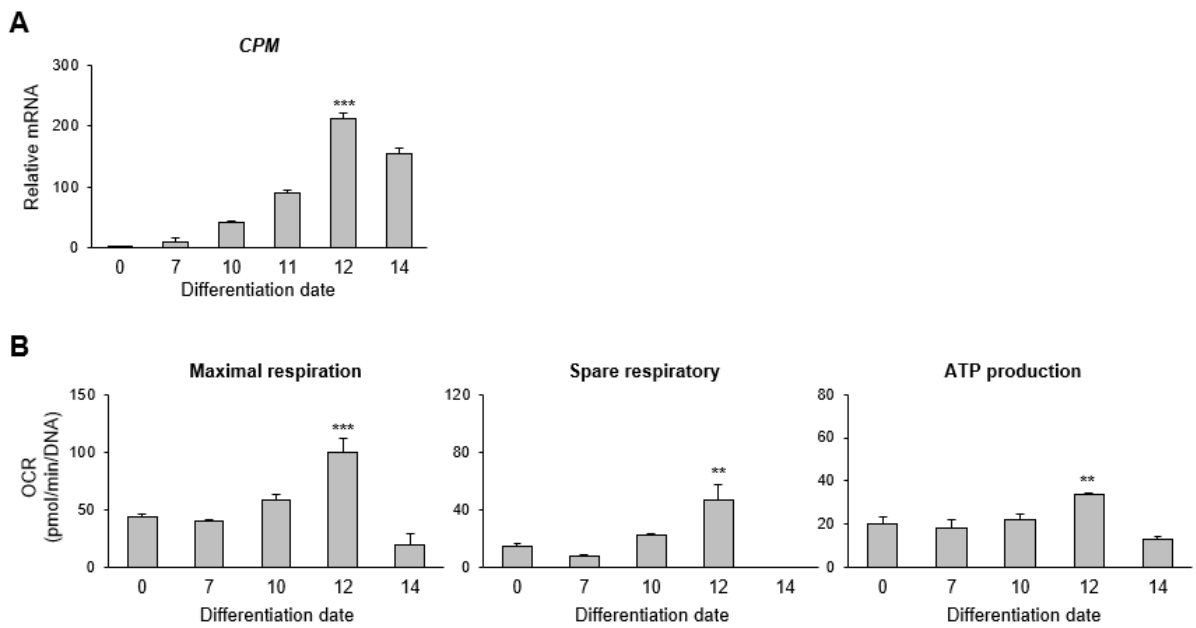


**Figure 16. Optimizing the differentiation date for transplantation.**

(A) Relative mRNA expression levels of hepatic progenitor marker (*CPM*) depending on the differentiation date. *GAPDH* was used as an internal control for RT-qPCR. (B) Oxygen consumption rates (OCR) according to the day of hepatic differentiation. OCR values were normalized by the DNA concentration. P-values < 0.05 were considered significant. \*, P < 0.05; \*\*, P < 0.01, \*\*\*, P < 0.001

### **III-4-3. Engraftability of AM-HPCs**

To confirm the engraftment of AM-HPCs, we transplanted half a million of AM-HPCs on different days 12 into the spleen of the NSG acute liver failure model. Three weeks later, the mice were examined (Figure. 14A). Three weeks after transplantation, human albumin was detected around the hepatic vein of the mouse liver with histological recovery (Figure. 14B).

We also tracked the transplanted cells by transfecting a green fluorescent protein (GFP) reporter gene to the AM-MSCs and confirmed that the GFP-expressions in AM-MSCs and day 12 AM-HPCs (Figure. 14C). As a result of transplantation, the ALB-positive cells were co-localized with GFP-expression (Figure. 14D). Additionally, we detected human mitochondrial DNA (mtDNA) in AM-HPC-transplanted liver tissue to confirm the success of transplantation. The human mtDNA was detected in the left lobe and the median lobe of the cell-transplanted liver tissue (Figure. 14E). We also confirmed by Sanger sequencing that the DNA sequences detected in the liver tissue were the same with injected AM-HPCs (Figure. 14F). In conclusion, day 12 AM-HPCs can be successfully engrafted into acute liver failure tissue, and remain long-term.

### **III-4-4. The therapeutic capacity of AM-HPCs**

Finally, we confirm the therapeutic effect of AM-HPCs. In histological analysis, the acute failure liver was displayed normal morphology after AM-HPCs transplantation (Figure. 15A). Moreover, we measured the survival rate of the mouse model. A total of 11 mice were inducted into the liver failure model. Two died on day 1, four died on day 2, and five died on day 3 after induction. As a result, the group of AM-HPCs transplantation was more survived than no transplantation group (Figure. 15B). Additionally, we analyzed the efficiency of transplantation using a standard curve of human and mouse mtDNA (Figure. 15C). The efficiency was approximately 6-12% human mtDNA present in the cell-transplanted mouse liver (Figure. 15D). These results suggest that AM-HPCs can successfully engraft in damaged livers and support regeneration.

### **III-4-5. Summary of *in vivo* studies**

In *in vivo* studies, we have successfully regenerated hepatocytes in the mouse model of acute liver failure using a newly developed method for HPC differentiated from human AM-MSCs (Figure. 16). To transplant and regenerate the acute liver failure, first, we optimized the date of transplantation by measuring the hepatic progenitor potent, *CPM*, and mitochondria function. Moreover, we developed a more robust mouse model using the chemicals, CTX and TAA. These made the mouse more suitable to

transplant the cells than when TAA was only used. Finally, we injected the cells into the spleen for liver transplantation and regeneration. Three weeks after transplantation, AM-HPCs were successfully transplanted into the acute failure liver, and the liver was recovered from the disease.

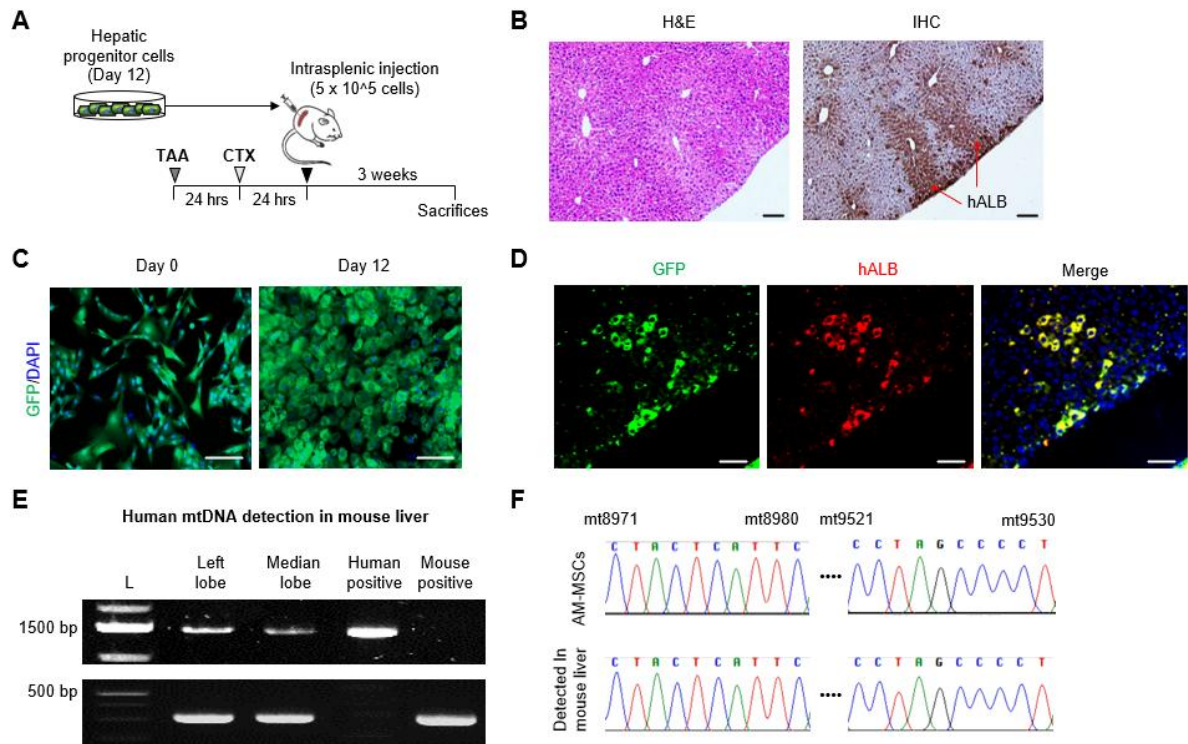


**Figure 17. AM-derived hepatic progenitor cells were successfully transplanted into an acute liver failure mouse model.**

(A) Schematic summary of transplantation experiments. To conduct the transplantation of AM-HPCs, NSG mice were used in this experiment. (B) H&E stain, and detection of human albumin by immunohistochemistry in transplanted mouse liver after three weeks. Scale bar = 50  $\mu$ m. (C) GFP-positive undifferentiated and differentiated cells. GFP was continuously expressed after differentiation. Scale bar = 200  $\mu$ m. (D) Confocal images of immunofluorescence stain for human albumin (red) with GFP (green). Nuclei were counterstained with DAPI (blue). Scale bar = 150  $\mu$ m. (E) Detection of human mitochondrial DNA in the mouse liver. Upper DNA gel: human mitochondrial DNA. Down DNA gel: mouse mitochondrial DNA. (F) Human mitochondrial DNA Sanger sequencing in AM-MSCs and AM-derived hepatic progenitor cells.

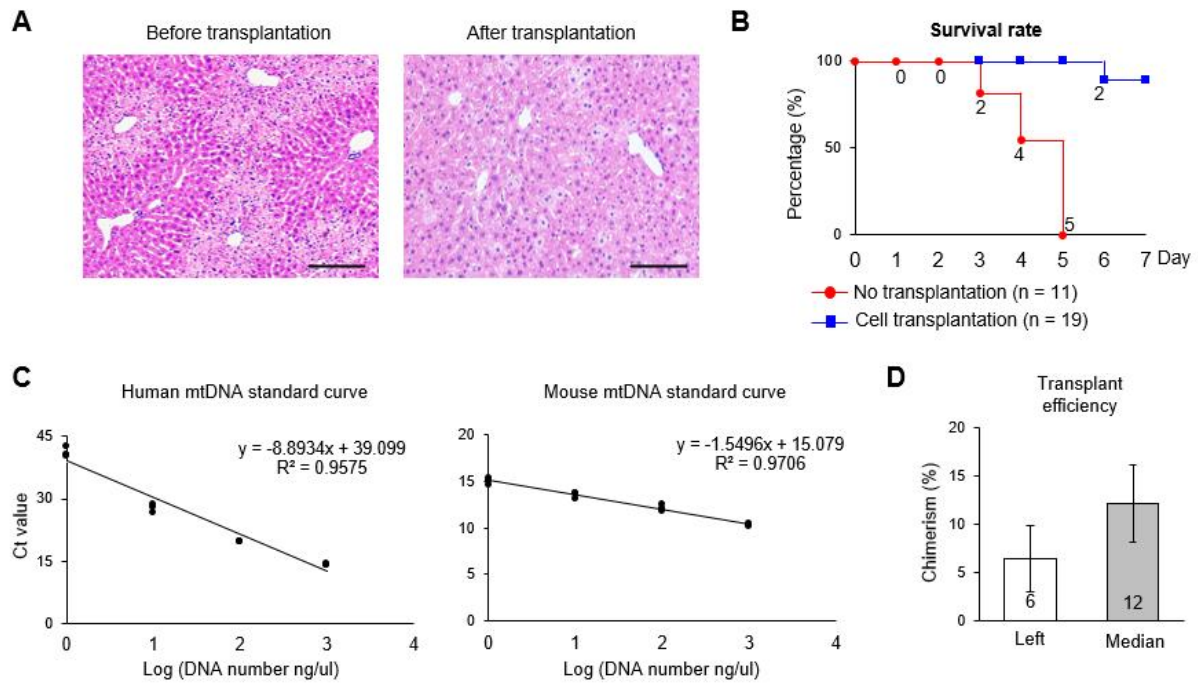


**Figure 18. The effect of AM-derived hepatic progenitor cells transplantation and efficiency.**

(A) H&E stain of before and after the cells transplantation. Scale bar = 200  $\mu$ m. (B) The survival rate of no transplantation and cell transplantation groups for 7 days. Number, the number of dead mice. (C) Standard curve of human and mouse mtDNA for calculating transfer efficiency. (D) Measurement of transplant efficiency using quantitative PCR with mouse and human mtDNA calibration curve. *GAPDH* was used as an internal control for RT-qPCR.

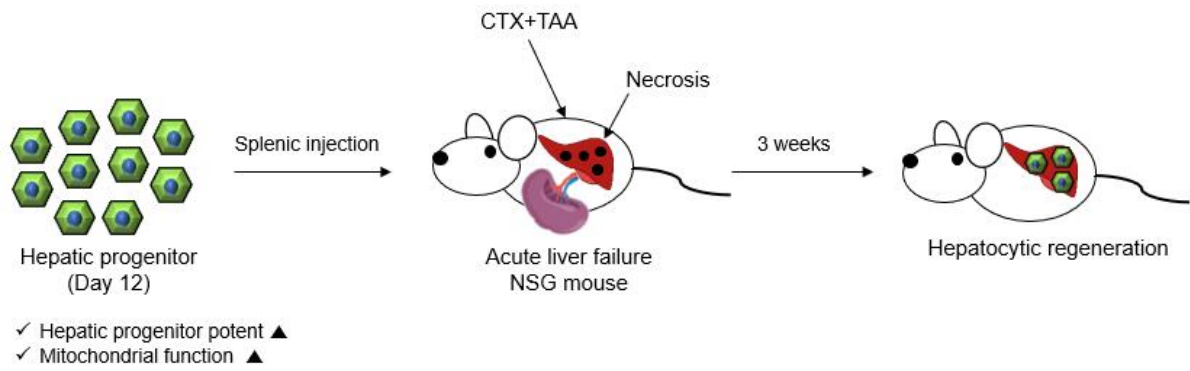


**Figure 19. Schematic summary of *in vivo* study.**



## Discussion

The advantage of stem cells for cell therapy would be safety, mass-producibility, and the ability to select the most effective cells. The ideal stem cells of the future are iPSCs, but there remain issues of safety and insufficient differentiation still exist [83]. In this study, we investigated the usual characteristics of UCM-MSCs, BM-MSCs, LD-MSCs, and AM-MSCs, and chose the one MSC line that was potentially used for cell therapy and differentiation according to the results of experiments.

In the aspect of size, LD-MSCs and AM-MSCs were smaller than other cell lines. A previous study reported that a large size of MSCs can be obstructed the bloodstream, and cause stroke [41]. Therefore, the two MSC lines had the advantage of cell size. We also measured the pluripotent-related genes, such as *OCT4*, *NANOG*, and *SOX2*, in the four different MSCs. In this aspect, *OCT4* was most highly expressed in AM-MSCs, while both *NANOG* and *SOX2* were highest in BM-MSCs. High expression levels of *OCT4* appeared that the stem cells could easily be transformed toward endoderm lineage under differentiation signals [84]. However, in chapter II, although AM-MSCs had the highest *OCT4* levels compared to other MSCs, they did not differentiate well into hepatocytes which were derived from endoderm. This result suggested that high expression levels of pluripotent-related genes do not imply a good capacity of differentiation into all types of cells. Next, we tested the immunomodulation of MSCs. In previous studies, MSCs release various anti-inflammation cytokines such as TGF $\beta$  and IL-10 and have a specific profile of major histocompatibility complex (MHC). Particularly, since MSCs were not expressed in MHC class II, T cell response is significantly reduced when MHC is injected into *in vivo* [85]. In our data, the profiles of inflammation cytokines were complicated. Therefore, we conducted the mixed lymphocyte reaction assay which can directly measure the immunomodulation capacity of MSCs *in vitro* [86]. As a result, LD-MSCs and AM-MSCs had better capacity than other MSCs. However, *in vivo* experiments should be conducted in order to conclude that LD-MSCs and AM-MSCs are modulated immune systems. In this experiment, we should use a humanized mouse, which is transplanted human peripheral blood mononuclear cells and produced human CD45-positive cells [87]. Therefore, further study is necessary for this part. We also measured the mitochondrial function in the UCM-MSCs, LD-MSCs, and AM-MSCs. Mitochondria are important organelles responsible for the energy metabolism in the cells. They can affect several functions of MSC, such as differentiation capacity [88]. However, it is not always correct. According to the results of chapter I, AM-MSCs had the best mitochondrial function. But, in the results of chapter II, AM-MSCs were not easily differentiated into HLCs.

The various stem cells derived from adult or embryonic tissues differ in differentiation abilities

depending on the origin of the tissue and desired differentiated cell type. For example, AM-MSCs had similar characteristics to UCM-MSCs in terms of phenotype and neonatal origin but differed in gene expression. Thus, we realized that different differentiation protocols might be necessary depending on the origin of the cells.

The UCM-MSCs were previously reported that the cells already expressed hepatocyte-related genes and could easily differentiate into HLCs [61]. Moreover, because of their similar characteristics, UCM-MSCs can be the comparative control of AM-MSC's transcriptome analysis. As a result, the AM-MSCs have lower expression levels of endoderm transcription factors, such as *GATA6*, *EGF*, *AFP*, *FGF2*, and *c-JUN*, and higher expression levels of *GSK3*.

In previous studies, CHIR has been used for hepatic differentiation from PSCs [89], we hypothesized that the GSK-3 inhibitor, CHIR, might promote differentiation to HPCs from AM-MSCs. This study showed that CHIR induced the expression of *GATA6* and *SOX17*, which were necessary genes for stem cells to differentiate into hepatocytes. Probably, GSK3 inhibited by CHIR activated *GATA6* signaling, which upregulated the Wnt/ $\beta$ -catenin pathway, leading to the enhancement of the *SOX17* gene [65, 71, 72]. Therefore, CHIR99021 with the addition of supplements, the advanced protocol conferred robust differentiation ability on the AM-MSCs. Besides, the ROCK inhibitor, Y-27632, has been used for differentiating hiPSCs to HPCs and reprogramming mature hepatocytes to the HPCs [62, 63]. Fasudil is a known ROCK inhibitor and only approval for clinical and it is similar to Y-27632 for using cell culture and differentiation [67]. Thus, we applied fasudil for differentiating AM-MSCs. The other growth factors and chemicals such as EGF, FGF2, HGF, Dexa, ITS, Nico, 5-aza, and OSM might promote the differentiation of definitive endoderm into hepatic endoderm or hepatic progenitor cells based on previous reports [90, 91].

FBS can contaminate cells during cell culture and differentiation, resulting in the presence of xeno-antigens and infectious agents that can provoke graft-versus-host disease [92]. It can also lead to differences between batches [93]. Hence, FBS must be replaced with an alternative supplement to achieve therapeutic outcomes in patients, but its use is still popular for hepatic differentiation despite the risks associated with transplantation. Polyvinyl alcohol (PVA) is a water-soluble synthetic polymer and has been used as a substitute for bovine serum albumin (BSA) in culture media for mouse preimplantation embryos [94]. It is also used in various human cell expansion and differentiation procedures for therapeutic applications, including hepatic differentiation from PSCs [95-98]. Interestingly, PVA could not only replace FBS but also significantly improve the differentiation to HPCs of AM-MSCs.

Finally, AM-HLCs, which were differentiated by efficient protocol with PVA, successfully secreted the human albumin, and the hepatic enzyme in AM-HLCs, CYP3A4, was worked. However, to use for cell therapy, AM-HLCs need more functional studies, such as urea synthesis, and should be compared with PHH. It is possible to determine the exact cell statement of AM-HLCs by comparing them with PHH. Thus, in this respect, Further study is necessary.

As *in vivo* study models, we induced two chemicals (TAA and CTX) to cause liver failure in mice. In previous studies, TAA is widely used in hepatic disease studies in models. However, TAA-induced models have difficulties controlling because of side effects [99]. For this reason, mouse models were easily dead when TAA was used. In addition, the model was not well induced in a low dose of TAA. Therefore, we used CTX, which is also known as toxic to the liver, and expected that CTX can be affected by the stability and liver damage of the mouse model. Our studies showed that TAA with CTX-induced mice has significantly increased expression of the liver damage markers (ALT, AST-GOT), and successfully induced necrosis on mouse liver.

We also optimized the transplantation date. On day 12, differentiated cells were the best conditions in terms of the number of human albumin-positive cells in the mouse liver. As we expected this time was matched with higher expression of CPM and EPCAM and OCR levels of mitochondria suggesting useful as biomarkers for transplanting of HPCs.

We have successfully regenerated hepatocytes in a mouse model using a newly developed method for HPC differentiated from human AM-MSCs. However, we should be conducted *in vivo* functional study to confirm that the transplanted cells were functionally worked, such as detection of human albumin in the transplanted mouse blood. Previous studies reported that mature hepatocytes were secreted albumin protein into blood [100]. Thus, human albumin, which existed in the transplanted mouse blood, should be detected to confirm that functional AM-HPCs were successfully transplanted.

In this study, we suggested that AM-MSCs can be used for cell therapy and hepatic differentiation under newly developed protocols. However, there are still problems to be solved before applying to clinical trials. In order to translate AM-MSCs or AM-HPCs or AM-HLCs into clinical practice, it is necessary to manufacture and perform quality control according to current good manufacturing practices (cGMP) [101]. According to cGMP, the establishment of clinical-grade cells requires the implementation of a quality control system and the consistent documentation of the whole process, such as procurement of biological material, culture, and freezing to quality control testing and distribution. Moreover, every step of this process has to be validated and executed according to standard operating procedures [102]. In this aspect, we should be confirmed and validated the chemicals and

proteins, which used in this study, whether they can be used clinically. We also need to compare differentiated cells with PHH in various aspects. As shown in this study, the differentiated cells clearly functioned and expressed various genes, but their levels were very low compared to PHH. Therefore, it is necessary to develop a maturation protocol that made AM-HLCs similar to PHH and needs to standardize the function and gene expression of AM-HLCs, which are considered normal levels [103].

In conclusion, this study established a more effective hepatic differentiation protocol for AM-MSCs by analyzing transcriptome profiles. Moreover, our findings suggested that PVA can be a suitable alternative to FBS in the differentiation for clinical trials. Finally, the results of in vivo experiment-supported AM-HPCs can be repopulated in the acutely injured livers and were spontaneously rescued by liver failure. To sum up, this study highlights the fact that AM-MSC-derived HPCs are a promising resource for treating acute liver failure.

## References

1. Popper H, Schaffner F. Liver: structure and function. 1957.
2. Abdel-Misih SRZ, Bloomston M. Liver Anatomy. *Surgical Clinics of North America*. 2010;90(4):643-53.
3. Trefts E, Gannon M, Wasserman DH. The liver. *Current Biology*. 2017;27(21):R1147-R51.
4. Tsung A, Geller DA. Gross and cellular anatomy of the liver. *Molecular pathology of liver diseases: Springer*; 2011. p. 3-6.
5. Schulze RJ, Schott MB, Casey CA, Tuma PL, McNiven MA. The cell biology of the hepatocyte: A membrane trafficking machine. *J Cell Biol*. 2019;218(7):2096-112.
6. Arroyo V, García-Martínez R, Salvatella X. Human serum albumin, systemic inflammation, and cirrhosis. *J Hepatol*. 2014;61(2):396-407.
7. Levitt DG, Levitt MD. Human serum albumin homeostasis: a new look at the roles of synthesis, catabolism, renal and gastrointestinal excretion, and the clinical value of serum albumin measurements. *International journal of general medicine*. 2016;9:229-55.
8. Cameron JM, Bruno C, Parachalil DR, Baker MJ, Bonnier F, Butler HJ, et al. Chapter 10 - Vibrational spectroscopic analysis and quantification of proteins in human blood plasma and serum. In: Ozaki Y, Baranska M, Lednev IK, Wood BR, editors. *Vibrational Spectroscopy in Protein Research: Academic Press*; 2020. p. 269-314.
9. Messner DJ, Murray KF, Kowdley KV, editors. *Mechanisms of Hepatocyte Detoxification* 2012.
10. Danielson PB. The Cytochrome P450 Superfamily: Biochemistry, Evolution and Drug Metabolism in Humans. *Current Drug Metabolism*. 2002;3(6):561-97.
11. Lee WM, editor *Acute liver failure. Seminars in respiratory and critical care medicine*; 2012: Thieme Medical Publishers.
12. Jalan R, Moreau R, Kamath PS, Arroyo V. Acute-on-Chronic Liver Failure: A Distinct Clinical Condition. *Semin Liver Dis*. 2016;36(02):107-8.
13. Llovet JM, Kelley RK, Villanueva A, Singal AG, Pikarsky E, Roayaie S, et al. Hepatocellular carcinoma. *Nature Reviews Disease Primers*. 2021;7(1):6.
14. Friedman SL. Liver fibrosis -- from bench to bedside. *J Hepatol*. 2003;38 Suppl 1:S38-53.
15. Bataller R, Brenner DA. Liver fibrosis. *The Journal of clinical investigation*. 2005;115(2):209-18.
16. Ginès P, Krag A, Abraldes JG, Solà E, Fabrellas N, Kamath PS. Liver cirrhosis. *The Lancet*. 2021;398(10308):1359-76.

17. Kotlyar DS, Burke A, Campbell MS, Weinrieb RM. A critical review of candidacy for orthotopic liver transplantation in alcoholic liver disease. *The American journal of gastroenterology*. 2008;103(3):734-43; quiz 44.
18. Keeffe EB. Liver transplantation: Current status and novel approaches to liver replacement. *Gastroenterology*. 2001;120(3):749-62.
19. Lantieri L, Grimbert P, Ortonne N, Suberbielle C, Bories D, Gil-Vernet S, et al. Face transplant: long-term follow-up and results of a prospective open study. *The Lancet*. 2016;388(10052):1398-407.
20. Burra P, Bizzaro D, Ciccocioppo R, Marra F, Piscaglia AC, Porretti L, et al. Therapeutic application of stem cells in gastroenterology: an up-date. *World J Gastroenterol*. 2011;17(34):3870-80.
21. Zakrzewski W, Dobrzyński M, Szymonowicz M, Rybak Z. Stem cells: past, present, and future. *Stem Cell Research & Therapy*. 2019;10(1):68.
22. Chagastelles PC, Nardi NB. Biology of stem cells: an overview. *Kidney International Supplements*. 2011;1(3):63-7.
23. Liu G, David BT, Trawczynski M, Fessler RG. Advances in Pluripotent Stem Cells: History, Mechanisms, Technologies, and Applications. *Stem cell reviews and reports*. 2020;16(1):3-32.
24. Hossein Aghdaie M, Geramizadeh B, Azarpira N, Esfandiari E, Darai M, Rahsaz M, et al. Hepatocyte isolation from unused/rejected livers for transplantation: initial step toward hepatocyte transplantation, the first experience from iran. *Hepat Mon*. 2013;13(8):e10397-e.
25. Sauer V, Roy-Chowdhury N, Guha C, Roy-Chowdhury J. Induced pluripotent stem cells as a source of hepatocytes. *Current pathobiology reports*. 2014;2(1):11-20.
26. Baharvand H, Hashemi SM, Shahsavani M. Differentiation of human embryonic stem cells into functional hepatocyte-like cells in a serum-free adherent culture condition. *Differentiation*. 2008;76(5):465-77.
27. Wu XB, Tao R. Hepatocyte differentiation of mesenchymal stem cells. *Hepatobiliary & pancreatic diseases international : HBPD INT*. 2012;11(4):360-71.
28. Miyajima A, Tanaka M, Itoh T. Stem/Progenitor Cells in Liver Development, Homeostasis, Regeneration, and Reprogramming. *Cell stem cell*. 2014;14(5):561-74.
29. Saeedi P, Halabian R, Imani Fooladi AA. A revealing review of mesenchymal stem cells therapy, clinical perspectives and Modification strategies. *Stem Cell Investig*. 2019;6:34-.
30. Wei X, Yang X, Han ZP, Qu FF, Shao L, Shi YF. Mesenchymal stem cells: a new trend for cell

- therapy. *Acta pharmacologica Sinica*. 2013;34(6):747-54.
31. Wannemuehler TJ, Manukyan MC, Brewster BD, Rouch J, Poynter JA, Wang Y, et al. Advances in mesenchymal stem cell research in sepsis. *The Journal of surgical research*. 2012;173(1):113-26.
  32. Pittenger MF, Discher DE, Péault BM, Phinney DG, Hare JM, Caplan AI. Mesenchymal stem cell perspective: cell biology to clinical progress. *npj Regenerative Medicine*. 2019;4(1):22.
  33. Zhou T, Yuan Z, Weng J, Pei D, Du X, He C, et al. Challenges and advances in clinical applications of mesenchymal stromal cells. *Journal of Hematology & Oncology*. 2021;14(1):24.
  34. Cook D, Genever P. Regulation of mesenchymal stem cell differentiation. *Advances in experimental medicine and biology*. 2013;786:213-29.
  35. Kim J, Piao Y, Pak YK, Chung D, Han YM, Hong JS, et al. Umbilical cord mesenchymal stromal cells affected by gestational diabetes mellitus display premature aging and mitochondrial dysfunction. *Stem cells and development*. 2015;24(5):575-86.
  36. Lee J, Choi J, Kang S, Kim J, Lee R, So S, et al. Hepatogenic Potential and Liver Regeneration Effect of Human Liver-derived Mesenchymal-Like Stem Cells. *Cells*. 2020;9(6).
  37. Zhang Q, Shi S, Liu Y, Uyanne J, Shi Y, Shi S, et al. Mesenchymal Stem Cells Derived from Human Gingiva Are Capable of Immunomodulatory Functions and Ameliorate Inflammation-Related Tissue Destruction in Experimental Colitis. *The Journal of Immunology*. 2009;183(12):7787.
  38. McCorry MC, Puetzer JL, Bonassar LJ. Characterization of mesenchymal stem cells and fibrochondrocytes in three-dimensional co-culture: analysis of cell shape, matrix production, and mechanical performance. *Stem Cell Research & Therapy*. 2016;7(1):39.
  39. Maleki M, Ghanbarvand F, Reza Behvarz M, Ejtemaei M, Ghadirkhomi E. Comparison of mesenchymal stem cell markers in multiple human adult stem cells. *Int J Stem Cells*. 2014;7(2):118-26.
  40. Zhang H, Menzies KJ, Auwerx J. The role of mitochondria in stem cell fate and aging. *Development*. 2018;145(8).
  41. Ge J, Guo L, Wang S, Zhang Y, Cai T, Zhao RCH, et al. The Size of Mesenchymal Stem Cells is a Significant Cause of Vascular Obstructions and Stroke. *Stem cell reviews and reports*. 2014;10(2):295-303.
  42. Weiss ARR, Dahlke MH. Immunomodulation by Mesenchymal Stem Cells (MSCs): Mechanisms of Action of Living, Apoptotic, and Dead MSCs. 2019;10(1191).

43. Boyer LA, Lee TI, Cole MF, Johnstone SE, Levine SS, Zucker JP, et al. Core Transcriptional Regulatory Circuitry in Human Embryonic Stem Cells. *Cell*. 2005;122(6):947-56.
44. Kabat M, Bobkov I, Kumar S, Grumet M. Trends in mesenchymal stem cell clinical trials 2004-2018: Is efficacy optimal in a narrow dose range? 2020;9(1):17-27.
45. Zetsche B, Heidenreich M, Mohanraju P, Fedorova I, Kneppers J, DeGennaro EM, et al. Multiplex gene editing by CRISPR-Cpf1 using a single crRNA array. *Nat Biotechnol*. 2017;35(1):31-4.
46. Vonderheide RH. CD47 blockade as another immune checkpoint therapy for cancer. *Nature Medicine*. 2015;21(10):1122-3.
47. Si-Tayeb K, Lemaigre FP, Duncan SA. Organogenesis and Development of the Liver. *Developmental Cell*. 2010;18(2):175-89.
48. Ober EA, Lemaigre FP. Development of the liver: Insights into organ and tissue morphogenesis. *Journal of Hepatology*. 2018;68(5):1049-62.
49. Kanai-Azuma M, Kanai Y, Gad JM, Tajima Y, Taya C, Kurohmaru M, et al. Depletion of definitive gut endoderm in Sox17-null mutant mice. *Development*. 2002;129(10):2367-79.
50. McLean AB, D'Amour KA, Jones KL, Krishnamoorthy M, Kulik MJ, Reynolds DM, et al. Activin A Efficiently Specifies Definitive Endoderm from Human Embryonic Stem Cells Only When Phosphatidylinositol 3-Kinase Signaling Is Suppressed. *Stem cells (Dayton, Ohio)*. 2007;25(1):29-38.
51. Miyajima A, Kinoshita T, Tanaka M, Kamiya A, Mukouyama Y, Hara T. Role of Oncostatin M in hematopoiesis and liver development. *Cytokine & growth factor reviews*. 2000;11(3):177-83.
52. Banas A, Teratani T, Yamamoto Y, Tokuhara M, Takeshita F, Osaki M, et al. Rapid hepatic fate specification of adipose-derived stem cells and their therapeutic potential for liver failure. *Journal of gastroenterology and hepatology*. 2009;24(1):70-7.
53. Chen J-Y, Mou X-Z, Du X-C, Xiang C. Comparative analysis of biological characteristics of adult mesenchymal stem cells with different tissue origins. *Asian Pacific Journal of Tropical Medicine*. 2015;8(9):739-46.
54. Ota M, Takagaki K, Takaoka S, Tanemura H, Urushihata N. A new method to confirm the absence of human and animal serum in mesenchymal stem cell culture media. *International Journal of Medical Sciences*. 2019;16(8):1102-6.
55. Jung S, Panchalingam KM, Rosenberg L, Behie LA. *Ex Vivo* Expansion of Human



- Mesenchymal Stem Cells in Defined Serum-Free Media. *Stem Cells International*. 2012;2012:123030.
56. Koivisto H, Hyvärinen M, Strömberg A-M, Inzunza J, Matilainen E, Mikkola M, et al. Cultures of human embryonic stem cells: serum replacement medium or serum-containing media and the effect of basic fibroblast growth factor. 2004;9(3):330-7.
  57. Inzunza J, Gertow K, Strömberg MA, Matilainen E, Blennow E, Skottman H, et al. Derivation of human embryonic stem cell lines in serum replacement medium using postnatal human fibroblasts as feeder cells. 2005;23(4):544-9.
  58. Galetin A, Ito K, Hallifax D, Houston JB. CYP3A4 Substrate Selection and Substitution in the Prediction of Potential Drug-Drug Interactions. *Journal of Pharmacology and Experimental Therapeutics*. 2005;314(1):180.
  59. Lee KS, Kim SK. Direct and metabolism-dependent cytochrome P450 inhibition assays for evaluating drug-drug interactions. *Journal of applied toxicology : JAT*. 2013;33(2):100-8.
  60. Zaret KS. Hepatocyte differentiation: from the endoderm and beyond. *Current opinion in genetics & development*. 2001;11(5):568-74.
  61. Campard D, Lysy PA, Najimi M, Sokal EM. Native Umbilical Cord Matrix Stem Cells Express Hepatic Markers and Differentiate Into Hepatocyte-like Cells. *Gastroenterology*. 2008;134(3):833-48.
  62. Morrison G, Scognamiglio R, Trumpp A, Smith A. Convergence of cMyc and  $\beta$ -catenin on Tcf7l1 enables endoderm specification. 2016;35(3):356-68.
  63. Zhao R, Watt AJ, Li J, Luebke-Wheeler J, Morrissey EE, Duncan SA. GATA6 Is Essential for Embryonic Development of the Liver but Dispensable for Early Heart Formation. *Molecular and Cellular Biology*. 2005;25(7):2622.
  64. Yang J, Lu P, Li M, Yan C, Zhang T, Jiang W. GATA6-AS1 Regulates GATA6 Expression to Modulate Human Endoderm Differentiation. *Stem Cell Reports*. 2020;15(3):694-705.
  65. Duda P, Akula SM, Abrams SL, Steelman LS, Martelli AM, Cocco L, et al. Targeting GSK3 and Associated Signaling Pathways Involved in Cancer. *Cells*. 2020;9(5).
  66. Michalopoulos GK, Bowen WC, Mulè K, Luo J. HGF-, EGF-, and dexamethasone-induced gene expression patterns during formation of tissue in hepatic organoid cultures. *Gene Expr*. 2003;11(2):55-75.
  67. So S, Lee Y, Choi J, Kang S, Lee J-Y, Hwang J, et al. The Rho-associated kinase inhibitor fasudil can replace Y-27632 for use in human pluripotent stem cell research. *PLOS ONE*.

- 2020;15(5):e0233057.
68. Afshari A, Shamdani S, Uzan G, Naserian S, Azarpira N. Different approaches for transformation of mesenchymal stem cells into hepatocyte-like cells. *Stem Cell Research & Therapy*. 2020;11(1):54.
  69. Zabulica M, Srinivasan RC, Vosough M, Hammarstedt C, Wu T, Gramignoli R, et al. Guide to the Assessment of Mature Liver Gene Expression in Stem Cell-Derived Hepatocytes. *Stem cells and development*. 2019;28(14):907-19.
  70. Drocourt L, Ourlin J-C, Pascussi J-M, Maurel P, Vilarem M-JJJoBC. Expression of cyp3a4, cyp2b6, and cyp2c9 is regulated by the vitamin d receptor pathway in primary human hepatocytes. 2002;277(28):25125-32.
  71. Tiyaboonchai A, Cardenas-Diaz FL, Ying L, Maguire JA, Sim X, Jobaliya C, et al. GATA6 Plays an Important Role in the Induction of Human Definitive Endoderm, Development of the Pancreas, and Functionality of Pancreatic  $\beta$  Cells. *Stem Cell Reports*. 2017;8(3):589-604.
  72. Huang J, Guo X, Li W, Zhang H. Activation of Wnt/ $\beta$ -catenin signalling via GSK3 inhibitors direct differentiation of human adipose stem cells into functional hepatocytes. *Scientific reports*. 2017;7:40716-.
  73. van der Spoel TIG, Jansen of Lorkeers SJ, Agostoni P, van Belle E, Gyöngyösi M, Sluijter JPG, et al. Human relevance of pre-clinical studies in stem cell therapy: systematic review and meta-analysis of large animal models of ischaemic heart disease. *Cardiovascular Research*. 2011;91(4):649-58.
  74. Marcellin P, Kutala BK. Liver diseases: A major, neglected global public health problem requiring urgent actions and large-scale screening. *Liver international : official journal of the International Association for the Study of the Liver*. 2018;38 Suppl 1:2-6.
  75. Akhtar T, Sheikh NJTR. An overview of thioacetamide-induced hepatotoxicity. 2013;32(3):43-6.
  76. Nevzorova YA, Boyer-Diaz Z, Cubero FJ, Gracia-Sancho J. Animal models for liver disease &#x2013; A practical approach for translational research. *Journal of Hepatology*. 2020;73(2):423-40.
  77. Bhat N, Kalthur SG, Padmashali S, Monappa VJEjohs. Toxic Effects of Different Doses of Cyclophosphamide on Live. 2018;28(6).
  78. Suzuki S, Toledo-Pereyra LH, Rodriguez FJ, Cejalvo D. Neutrophil infiltration as an important factor in liver ischemia and reperfusion injury. Modulating effects of FK506 and cyclosporine.

- Transplantation. 1993;55(6):1265-72.
79. Wallace MC, Hamesch K, Lunova M, Kim Y, Weiskirchen R, Strnad P, et al. Standard operating procedures in experimental liver research: thioacetamide model in mice and rats. *Laboratory animals*. 2015;49(1 Suppl):21-9.
  80. SELL S. The role of progenitor cells in repair of liver injury and in liver transplantation. *2001;9(6):467-82*.
  81. Kido T, Kouji Y, Suzuki K, Kobayashi A, Miura Y, Chern EY, et al. CPM Is a Useful Cell Surface Marker to Isolate Expandable Bi-Potential Liver Progenitor Cells Derived from Human iPS Cells. *Stem cell reports*. 2015;5(4):508-15.
  82. Choi SW, Gerencser AA, Nicholls DG. Bioenergetic analysis of isolated cerebrocortical nerve terminals on a microgram scale: spare respiratory capacity and stochastic mitochondrial failure. *Journal of Neurochemistry*. 2009;109(4):1179-91.
  83. Andrews PW, Ben-David U, Benvenisty N, Coffey P, Eggan K, Knowles BB, et al. Assessing the Safety of Human Pluripotent Stem Cells and Their Derivatives for Clinical Applications. *Stem Cell Reports*. 2017;9(1):1-4.
  84. Pan GJ, Chang ZY, SchÖLer HR, Pei D. Stem cell pluripotency and transcription factor Oct4. *Cell Research*. 2002;12(5):321-9.
  85. Weiss ARR, Dahlke MH. Immunomodulation by Mesenchymal Stem Cells (MSCs): Mechanisms of Action of Living, Apoptotic, and Dead MSCs. *Front Immunol*. 2019;10:1191-.
  86. Nicotra T, Desnos A, Halimi J, Antonot H, Reppel L, Belmas T, et al. Mesenchymal stem/stromal cell quality control: validation of mixed lymphocyte reaction assay using flow cytometry according to ICH Q2(R1). *Stem Cell Research & Therapy*. 2020;11(1):426.
  87. Walsh NC, Kenney LL, Jangalwe S, Aryee KE, Greiner DL, Brehm MA, et al. Humanized Mouse Models of Clinical Disease. *Annual review of pathology*. 2017;12:187-215.
  88. Yan W, Diao S, Fan Z. The role and mechanism of mitochondrial functions and energy metabolism in the function regulation of the mesenchymal stem cells. *Stem Cell Research & Therapy*. 2021;12(1):140.
  89. Hannoun Z, Steichen C, Dianat N, Weber A, Dubart-Kupperschmitt A. The potential of induced pluripotent stem cell derived hepatocytes. *Journal of Hepatology*. 2016;65(1):182-99.
  90. Campard D, Lysy PA, Najimi M, Sokal EM. Native umbilical cord matrix stem cells express hepatic markers and differentiate into hepatocyte-like cells. *Gastroenterology*. 2008;134(3):833-48.

91. Okura H, Komoda H, Saga A, Kakuta-Yamamoto A, Hamada Y, Fumimoto Y, et al. Properties of hepatocyte-like cell clusters from human adipose tissue-derived mesenchymal stem cells. *Tissue engineering Part C, Methods*. 2010;16(4):761-70.
92. Oikonomopoulos A, van Deen WK, Manansala A-R, Lacey PN, Tomakili TA, Ziman A, et al. Optimization of human mesenchymal stem cell manufacturing: the effects of animal/xeno-free media. *Scientific Reports*. 2015;5(1):16570.
93. Haque N, Kasim NHA, Rahman MT. Optimization of Pre-transplantation Conditions to Enhance the Efficacy of Mesenchymal Stem Cells. *International Journal of Biological Sciences*. 2015;11(3):324-34.
94. Biggers J, Summers M, McGinnis L. Polyvinyl alcohol and amino acids as substitutes for bovine serum albumin in culture media for mouse preimplantation embryos. *Human reproduction update*. 1997;3(2):125-35.
95. Wilkinson AC, Ishida R, Kikuchi M, Sudo K, Morita M, Crisostomo RV, et al. Long-term ex vivo haematopoietic-stem-cell expansion allows nonconditioned transplantation. *Nature*. 2019;571(7763):117-21.
96. Stocco E, Barbon S, Lora L, Grandi F, Sartore L, Tiengo C, et al. Partially oxidized polyvinyl alcohol conduit for peripheral nerve regeneration. *Sci Rep*. 2018;8(1):604.
97. Burridge PW, Thompson S, Millrod MA, Weinberg S, Yuan X, Peters A, et al. A universal system for highly efficient cardiac differentiation of human induced pluripotent stem cells that eliminates interline variability. 2011;6(4).
98. Nishimura T, Hsu I, Martinez-Krams DC, Nakauchi Y, Majeti R, Yamazaki S, et al. Use of polyvinyl alcohol for chimeric antigen receptor T-cell expansion. *Experimental hematology*. 2019;80:16-20.
99. Wallace M, Hamesch K, Lunova M, Kim Y, Weiskirchen R, Strnad P, et al. Standard operating procedures in experimental liver research: thioacetamide model in mice and rats. 2015;49(1\_suppl):21-9.
100. Buyl K, De Kock J, Bolleyn J, Rogiers V, Vanhaecke T. Measurement of Albumin Secretion as Functionality Test in Primary Hepatocyte Cultures. *Methods in molecular biology (Clifton, NJ)*. 2015;1250:303-8.
101. Sensebé L, Gadelorge M, Fleury-Cappellesso SJSCR, Therapy. Production of mesenchymal stromal/stem cells according to good manufacturing practices: a review. 2013;4(3):1-6.
102. Rehakova D, Souralova T, Koutna I. Clinical-Grade Human Pluripotent Stem Cells for Cell

- Therapy: Characterization Strategy. *Int J Mol Sci.* 2020;21(7):2435.
103. Schwartz RE, Fleming HE, Khetani SR, Bhatia SN. Pluripotent stem cell-derived hepatocyte-like cells. *Biotechnol Adv.* 2014;32(2):504-13.